Journal of Symbolic Computation 115 (2023) 452–477

Contents lists available at ScienceDirect

Journal of Symbolic Computation

www.elsevier.com/locate/jsc

Signatures of algebraic curves via numerical algebraic geometry

Timothy Duff [a], Michael Ruddy [b]

[a] Department of Mathematics, University of Washington, United States of America
[b] University of San Francisco, United States of America

ARTICLE INFO

Article history:
Available online 5 August 2022

Keywords:
Differential invariants
Invariant theory
Numerical algebraic geometry
Euclidean group
Computer algebra
Homotopy continuation

ABSTRACT

We apply numerical algebraic geometry to the invariant-theoretic problem of detecting symmetries between two plane algebraic curves. We describe an efficient equality test which determines, with "probability-one", whether or not two rational maps have the same image up to Zariski closure. The application to invariant theory is based on the construction of suitable signature maps associated to a group acting linearly on the respective curves. We consider two versions of this construction: differential and joint signature maps. In our examples and computational experiments, we focus on the complex Euclidean group, and introduce an algebraic joint signature that we prove determines equivalence of curves under this action and the size of a curve's symmetry group. We demonstrate that the test is efficient and use it to empirically compare the sensitivity of differential and joint signatures to different types of noise.

1. Introduction

The study of plane curves under linear group actions is a classical subject of both differential (Guggenheimer, 1963) and algebraic geometry (Olver, 1999) with applications to image science (Mundy et al., 1994). In particular, an important problem is to determine whether two curves are equivalent under such a group action, which is more difficult when there is a significant level of

E-mail addresses: timduff@uw.edu (T. Duff), mruddy@usfca.edu (M. Ruddy).

https://doi.org/10.1016/j.jsc.2022.08.003
0747-7171/

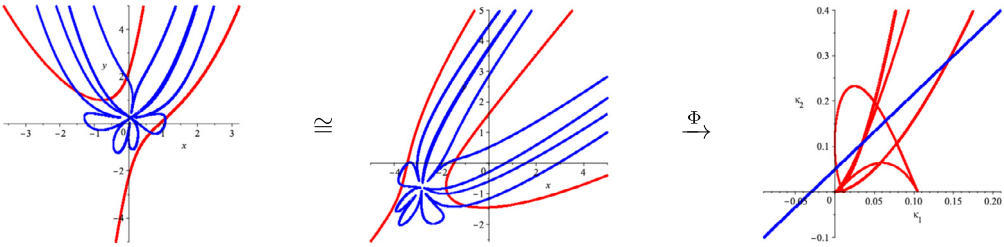

Fig. 1. Two $\mathcal{E}_2(\mathbb{C})$-equivalent curves and their differential signature curve in red. A line and its pullback under the respective signature maps in blue. (For interpretation of the colors in the figures, the reader is referred to the web version of this article.)

noise. For instance, when the transformation group is the group of rigid motions, this can translate to deciding whether two contours represent the same object in different positions, or, in the case of affine and projective transformations, whether two contours might correspond to different projections of the same 3D object. For plane algebraic curves, we state the *group equivalence problem* as follows ($\overline{\bullet}$ denotes Zariski closure):

Problem 1. Given a positive dimensional algebraic group $G \subset \mathcal{PGL}_3(\mathbb{C})$ acting linearly on $\mathbb{C}^2$ and two plane algebraic curves $C_0, C_1 \subset \mathbb{C}^2$, decide if there exists $g \in G$ such that $C_0 = \overline{g \cdot C_1}$.

There exist many different symbolic algorithms to determine equivalence under a particular group of algebraic transformations. For instance, one can directly use elimination algorithms to determine whether there exists such a group element. One can also use invariants, for example by constructing a set of rational invariants that characterize the orbits of the action on the coefficients of curves of fixed degree d (Derksen and Kemper, 2015; Hubert and Kogan, 2007; Sturmfels, 2008) or by constructing a pair of rational differential invariants which define a signature polynomial on a curve characterizing its equivalence class (Burdis et al., 2013; Kogan et al., 2020).

In the analogous setting of *smooth* curves in $\mathbb{R}^2$, the Fels-Olver moving frame method (Fels and Olver, 1999), based on Cartan's method of moving frames, associates to each curve a *differential signature curve*, defined in terms of smooth invariants, which is classifying for the group action. In greater generality, differential signatures may be constructed for smooth submanifolds of some ambient space equipped with a Lie group action. The differential signature locally characterizes the manifold's equivalence class under the action, meaning that manifolds with the same signature are locally equivalent under the Lie group (Fels and Olver, 1999). Differential signatures of curves have been successfully applied to object recognition under noise, where it seems that curves that are "almost" equivalent have "close" signatures. Specific applications range from jigsaw puzzle reconstruction (Hoff and Olver, 2014) to medical imaging (Grim and Shakiban, 2017). They have also been used to solve classical invariant theory problems such as determining equivalence of binary and ternary forms (Berchenko (Kogan) and Olver, 2000; Kogan and Moreno Maza, 2002; Olver, 1999).

Differential signatures were adapted from the smooth setting in order to construct explicit algebraic invariants in Hubert and Kogan (2007) and rational invariants in Kogan et al. (2020) for plane algebraic curves. In Burdis et al. (2013) the notion of a signature polynomial was introduced to determine equivalence of plane algebraic curves, and in Kogan et al. (2020) it is shown that this reduction to Problem 2 can always be done. For our purposes, the differential signature curve of an affine curve $C \subset \mathbb{C}^2$ with respect to some group action will always be the image of some rational map $\Phi : C \dashrightarrow \mathbb{C}^2$.

Example 1.1. In Fig. 1, the red curve on left depicts real points (x, y) satisfying the cubic equation $8x^3 - 20xy + 2y^2 + 5x - 10 = 0$. Applying a real rotation and translation yields the red curve in the middle. Theorem 2.18 tells us that they have the same differential signature curve. This is a degree 48 curve, depicted in red on the right.

In the setting of Problem 1, Kogan et al. (2020) observed that local equivalence implies global equivalence, reducing Problem 1 to a special case of Problem 2 below.

Problem 2. Given two irreducible algebraic varieties, $X_0 \subset \mathbb{C}^{n_0}$ and $X_1 \subset \mathbb{C}^{n_1}$, and rational maps, $\Phi_0 : X_0 \dashrightarrow \mathbb{C}^m$ and $\Phi_1 : X_1 \dashrightarrow \mathbb{C}^m$, decide if $\overline{\operatorname{im}\Phi_0} = \overline{\operatorname{im}\Phi_1}$.[1]

In the smooth setting, the reduction of Problem 1 to Problem 2 can also be achieved through the use of *joint signatures* (introduced in Olver, 2001) which are obtained by constructing maps using joint invariants of the induced action of G on the product $\mathbb{C}^2 \times \ldots \times \mathbb{C}^2$. The joint signatures may be interpreted as 0-th order differential invariants, and are considered to be more noise-resistant in applications. This further motivates our interest in studying Problem 2 in full generality.

In this paper, we study the group equivalence problem for the complex Euclidean group $\mathcal{E}_2(\mathbb{C})$ via differential and joint signatures. As a theoretical contribution, we complement the results of Kogan et al. (2020) (summarized in Section 2.2) with a rigorous analysis of Euclidean joint signatures, which characterize $\mathcal{E}_2(\mathbb{C})$-equivalence in our algebraic setting (Theorem 2.24). Another main contribution is our use of *numerical algebraic geometry*. This allows us to study the joint signature for curves of higher degree than symbolic methods would allow; as an upshot, we obtain a conjectural formula for the degree of the joint signature of a generic curve (see Conjecture 4.2). Numerical algebraic geometry also gives us a novel approach to Problem 2 (and hence also Problem 1) based on witness sets. To accommodate the many variations on the signature construction, we state a general algorithm for Problem 2; this equality test is a variation on the standard membership tests from numerical algebraic geometry. Admittedly, this approach is far less straightforward than the direct approach to Problem 1 in which the group element g is solved for directly. Our interest in numerical algebraic geometry is partially motivated by the potential viability of numerical methods in noisy settings. As a third contribution, we experimentally investigate the potential of the equality test for signatures to measure of "near-equivalence" of curves.

A previous version of this work appeared in the conference proceedings of ISSAC 2020 (Duff and Ruddy, 2020). In this version we have made significant revisions, with simpler proofs of the main results on joint signatures. We also include new results relating the curve's symmetry group to the joint signature (Proposition 2.31), which mirror previous results of Kogan et al. (2020) for the differential signature map. We conduct several new experiments on the sensitivity of the numerical equality test to noise, now involving the equi-affine group as well as curves computed from noisy samples. Finally, we include several new examples.

The paper is organized as follows. Section 2 gives a general overview of signatures and their relation to the group equivalence problem. In 2.2, we recall the results of Burdis et al. (2013), Kogan et al. (2020), where the differential signature for a plane algebraic curve is constructed using a *classifying pair* of differential invariants. In 2.3 we describe how joint signatures can be used to determine equivalence of plane curves using lower order differential invariant functions, and mirror these previous results for the particular case of the complex Euclidean group $\mathcal{E}_2(\mathbb{C})$. In Section 3, we review some notions from numerical algebraic geometry, before stating a general solution to Problem 2 (Algorithm 1) in Section 3.2, with additional comments relevant to the application to signatures in 3.3. In Section 4, we describe an implementation in Macaulay2 (Grayson and Stillman, 1997). Our experiments demonstrate that computing witness sets for plane curves of relatively high degree is feasible and that, for precomputed witness sets, the online equality test gives a fast alternative to symbolic methods for signatures, and that Finally, we observe our numerical approach is robust in a certain, moderate regime of noise in which we subject the curves to different types of perturbations. The experiments were conducted using version 1.17 of Macaulay2 (Grayson and Stillman, 1997); our implementation and scripts for running experiments may be obtained via the url https://github.com/timduff35/NumericalSignatures.

[1] In Problem 2, $\overline{\operatorname{im}\Phi_i}$ denotes the Zariski closure of the image of Φ_i. We do not address the more delicate problem of deciding equality of the constructible sets $\operatorname{im}\Phi_i$.

2. Signatures of curves

2.1. Invariants of plane curves

Invariants and the classification of differentiable curves in $\mathbb{R}^2$ with respect to rigid motions are classical subjects in differential geometry (Guggenheimer, 1963). This can be seen as a variant on what we defined as Problem 1.

Definition 2.1. Two curves C_0, C_1 are said to be *G-equivalent*, denoted $C_0 \cong_G C_1$, if there exists an element g in the group of transformations G such that $C_0 = g \cdot C_1$.

Remaining purposefully agnostic about what constitutes a "curve" and a "group of transformations," we can define the *Group equivalence problem for curves* as: given two curves and a group of transformations G decide if they are G-equivalent. In this context both classical questions about geometry of real curves and Problem 1 are both specific instances of a larger class of problems. In this subsection, we discuss how previous work on the group equivalence problem for differentiable curves in $\mathbb{R}^2$ connects to our approach to Problem 1 for algebraic curves in $\mathbb{C}^2$.

For now let C refer to the image of a smooth[2] map $\gamma = (x(t), y(t))$ where $\gamma : I \to \mathbb{R}^2$ for some interval $I \subset \mathbb{R}$. We denote $\mathcal{SE}_2(\mathbb{R})$ as the *special Euclidean group*, the transformation group of rotations and translations of $\mathbb{R}^2$. A classical invariant of curves under rigid motion is the Euclidean curvature function $\kappa(t)$, defined below in (1), meaning that the value of curvature at a particular point of a curve does not change when the curve transformed by $\mathcal{SE}_2(\mathbb{R})$.

$$\kappa(t) = \frac{x'(t)y''(t) - y'(t)x''(t)}{(x'(t)^2 + y'(t)^2)^{3/2}} \tag{1}$$

Euclidean curvature at a point on a curve can be defined in many "geometrically-satisfying" ways, as the multiplicative inverse of the radius of the osculating circle, or norm of the tangent vector when the curve is parameterized by arc length. Euclidean curvature also provides a way to solve the group equivalence problem for curves under $\mathcal{SE}_2(\mathbb{R})$. The following theorem appears in many places, for instance (Guggenheimer, 1963), and is sometimes referred to as the "Fundamental theorem for planar curves."

Theorem 2.2. *If two smooth curves have the same Euclidean curvature as a function of arc length, then they are $\mathcal{SE}_2(\mathbb{R})$-equivalent.*

Thus $\kappa(s)$, Euclidean curvature when C is parameterized by the arc length parameter s, completely determines a curve up to $\mathcal{SE}_2(\mathbb{R})$. In practice comparing curves' curvature functions to determine $\mathcal{SE}_2(\mathbb{R})$-equivalence is difficult as this comparison depends on the parameterization and the starting point when the curve is closed. In this sense, a single curve can have infinitely many different curvature functions. Motivated by applications to object recognition, the authors of Calabi et al. (1998) proposed the use of the *Euclidean signature curve* to determine $\mathcal{SE}_2(\mathbb{R})$-equivalence of smooth curves.

Definition 2.3. The *Euclidean signature curve* of a smooth curve C is the image of C under the map $\mathcal{S} : C \to \mathbb{R}^2$ defined by $\mathcal{S} = (\kappa, \kappa_s)$, where κ_s is the function representing the derivative of κ with respect to arc length.

Theorem 2.4 *(Theorem 2.3 in Calabi et al., 1998). If two smooth curves, C_0, C_1 have the same Euclidean signature curve, then they are locally equivalent under $\mathcal{SE}_2(\mathbb{R})$.*

[2] Here smooth refers to a map defined by infinitely differentiable functions. For simplicity we require smooth functions, though for the results and constructions referenced, this restriction can be loosened to n-differentiable for an appropriate choice of n.

Here locally equivalent means that around each point of C_0, there exist open subsets $U_0 \subset C_0$ and $U_1 \subset C_1$ such that $U_0 = g \cdot U_1$ for some $g \in \mathcal{SE}_2(\mathbb{R})$. Thus the local geometry of a curve is determined by the relationship between Euclidean curvature and another differential invariant function, the derivative of κ with respect to arc length. For closed curves this relationship is invariant with respect to parameterization and starting point. Intuitively this produces an object, the Euclidean signature, where curves with local geometries that are "close" have "close" signatures. The word "close" appears here in quotations as there is no rigorous statement to this effect, and a good definition of "close" in this context needs further investigation. Nevertheless this idea still led to subsequent works where the Euclidean signature curve is used for a curve matching algorithm (Hoff and Olver, 2013) and then applied to automatic jigsaw puzzle reassembly (Hoff and Olver, 2014).

The authors of Calabi et al. (1998) also note that this procedure generalizes to plane curves under other transformation groups of $\mathbb{R}^2$. For most Lie group actions of G on $\mathbb{R}^2$ there exists a notion of G-invariant curvature κ and G-invariant arc length s such that if curves have the same image, or *differential signature*, under (κ, κ_s) then they are locally equivalent under G (Calabi et al., 1998, Thm 5.2). Moreover a pair of such differential invariants can be constructed explicitly by the Fels-Olver moving frame method (Fels and Olver, 1999), giving a practical method to locally solve the group equivalence problem for smooth curves.

Turning attention back to Problem 1, for algebraic curves local equivalence under a group G immediately implies global G-equivalence as in Definition 2.1. Thus the differential signature characterizes algebraic curves under a transformation group G. In Burdis et al. (2013) the authors connect the differential signature to symbolic methods by noticing that when the differential invariants can be expressed as a rational map on the curve, two algebraic curves' differential signatures can be compared by computing their implicit equations, connecting Problem 2 to the group equivalence problem for algebraic curves over $\mathbb{R}^2$.

In Kogan et al. (2020) it is shown that for any subgroup of $\mathcal{PGL}_3(\mathbb{C})$ there exists a pair of rational differential invariants which can reduce Problem 1 to Problem 2. Thus the differential signature can be used to solve questions of classical invariant theory in a way that uses the same invariants regardless of the degree of the algebraic curves in question. Moreover these differential invariants can be interpreted as generators of a field of rational invariants, meaning that they can be computed by symbolic methods such as those in Derksen and Kemper (2015) or the cross-section method in Hubert and Kogan (2007) inspired by the previously mentioned moving frame method. Thus Problem 1 can be solved end-to-end by symbolic computation in this way.

In practice, these methods can be quite slow for computing implicit equations of differential signatures (see Ruddy (2019, Ex. 3.2.13) for instance), which is our motivation to further extend the connection between Problem 1 to Problem 2 by leveraging numerical algorithms for computing pseudo-witness sets to compare differential signatures of algebraic curves. In Section 2.2 we explain, in greater detail, the reduction of Problem 1 to Problem 2 along with examples.

In addition to differential invariants, a similar approach has been taken using *joint* differential invariants to solve the group equivalence problem for smooth curves in Olver (2001), which are in theory more robust to noise and perturbations. In Section 2.3 we consider for the first time using the joint signature in a completely algebraic approach to Problem 1, proving in the case of $\mathcal{E}_2(\mathbb{C})$ that the Euclidean joint signature characterizes equivalence classes of algebraic curves.

In the next two sections, we assume that plane curves are complex algebraic, irreducible, and of degree greater than one. The degree restriction removes from consideration lines, on which not all transformations $g \in G$ may not be defined.

2.2. Differential signatures

For algebraic curves, we tweak Definition 2.1 to the following definition, which allows for the image of a curve under the action of G to not be closed.

Definition 2.5. Two algebraic curves C_1 and C_2 are *G-equivalent* if there exists $g \in G$ such that $C_1 = \overline{g \cdot C_2}$.

We assume that the group $G \subset \mathcal{PGL}_3(\mathbb{C})$ is a positive dimensional algebraic group acting linearly on $\mathbb{C}^2$ with action $g \cdot (x, y) = (\overline{x}, \overline{y})$.

Definition 2.6. The *projective group* $\mathcal{PGL}_3(\mathbb{C})$ is the group of invertible matrices modulo scaling, i.e. $\mathcal{PGL}_3(\mathbb{C}) \cong {}^{\mathcal{GL}_3(\mathbb{C})}\!/_{\lambda I}$. The linear action on $\mathbb{C}^2$ is defined by the map $\Phi : \mathcal{PGL}_3(\mathbb{C}) \times \mathbb{C}^2 \dashrightarrow \mathbb{C}^2$ where for $A \in \mathcal{PGL}_3(\mathbb{C})$ and $p = (x, y) \in \mathbb{C}^2$,

$$\Phi(A, p) = \left(\frac{a_{11}x + a_{12}y + a_{13}}{a_{31}x + a_{32}y + a_{33}}, \frac{a_{21}x + a_{22}y + a_{23}}{a_{31}x + a_{32}y + a_{33}} \right).$$

We consider a few classical subgroups of $\mathcal{PGL}_3(\mathbb{C})$.

Definition 2.7. The *Euclidean group* $\mathcal{E}_2(\mathbb{C})$ is the subgroup of $\mathcal{PGL}_3(\mathbb{C})$ given by matrices of the form

$$\begin{bmatrix} \alpha c & \alpha s & a \\ -s & c & b \\ 0 & 0 & 1 \end{bmatrix}$$

where $a, b, c, s \in \mathbb{C}$, $\alpha \in \{-1, 1\}$, and $c^2 + s^2 = 1$.

Definition 2.8. The *special Euclidean group* $\mathcal{SE}_2(\mathbb{C})$ is the subgroup of $\mathcal{E}_2(\mathbb{C})$ consisting of determinant one matrices.

Definition 2.9. The *equi-affine group* $\mathcal{SA}_2(\mathbb{C})$ is the subgroup of $\mathcal{PGL}_3(\mathbb{C})$ given by matrices of the form

$$\begin{bmatrix} a_{11} & a_{12} & a_{13} \\ a_{21} & a_{22} & a_{23} \\ 0 & 0 & 1 \end{bmatrix}$$

with entries in $\mathbb{C}$ and $a_{11}a_{22} - a_{12}a_{21} = 1$.

A differential signature that determines G-equivalence of algebraic curves can be constructed from a set of classifying invariants (Definition 2.15). We let J^n denote the nth order jet space, a complex vector space of dimension $(n+2)$ with coordinates $(x, y, y^{(1)}, \ldots, y^{(n)})$. Letting $\Omega(J^n)$ denote the set of complex-differentiable functions from J^n to $\mathbb{C}$, the *total derivative operator* $\frac{d}{dx} : \Omega(J^n) \to \Omega(J^{n+1})$ is the unique $\mathbb{C}$-linear map satisfying the product rule and the relations $\frac{d}{dx}(x) = 1$, $\frac{d}{dx}(y^{(k)}) = y^{(k+1)}$ for $k \geq 0$, cf. Olver (1995, Ch. 7). The *prolonged* action of G on J^n is given by

$$g \cdot (x, y, y^{(1)}, \ldots, y^{(n)}) = (\overline{x}, \overline{y}, \overline{y}^{(1)}, \ldots, \overline{y}^{(n)})$$

where

$$\overline{y}^{(1)} = \frac{\frac{d}{dx}[\overline{y}(g, x, y)]}{\frac{d}{dx}[\overline{x}(g, x, y)]}, \quad \overline{y}^{(k+1)} = \frac{\frac{d}{dx}\left[\overline{y}^{(k)}(g, x, y, y^{(1)}, \ldots, y^{(k)})\right]}{\frac{d}{dx}[\overline{x}(g, x, y)]} \text{ for } k = 1, \ldots, n-1.$$

Definition 2.10. A *differential invariant* for the action of G is a function on J^n that is invariant under the prolonged action of G on J^n. The *order* of a differential invariant is the maximum k such that the function depends explicitly on $y^{(k)}$.

Definition 2.11. The *n-th jet* of an algebraic curve C is the image of the map $j^n_C : C \dashrightarrow J^n$ given (where defined) by

$$(x, y) \mapsto (x, y, y_C^{(1)}(x, y), y_C^{(2)}(x, y), \ldots, y_C^{(n)}(x, y)),$$

where $y_C^{(k)}(x, y)$ is the k-th derivative of y with respect to x at the point $(x, y) \in C$.

The prolonged action of G is defined such that

$$g \cdot j_C^n(C) = j_{g\cdot C}^n(g \cdot C).$$

Definition 2.12. The *restriction* of a differential invariant K of order n to a curve C is the map $K|_C : C \dashrightarrow \mathbb{C}^2$ given by $K|_C = K \circ j_C^n$.

The coordinates of the n-th jet map j_C^n are rational functions of x and y that can be computed via implicit differentiation:

$$y_C^{(1)} = \frac{-\partial_x F}{\partial_y F} \quad \text{and} \quad y_C^{(k+1)} = \partial_x y_C^{(k)} + \partial_y y_C^{(k)} y_C^{(1)}, \tag{2}$$

where $\mathcal{I}_C = \langle F \rangle$. Thus, if K is a *rational* differential invariant of order n, meaning it is a rational function in the coordinates of J^n, then $K|_C$ is a rational function in x and y.

Definition 2.13. We say that a set of differential invariants $\mathcal{I}$ *separates orbits* for the prolonged action on a nonempty Zariski-open $W \subset J^n$ if, for all $p, q \in W$,

$$K(p) = K(q) \ \forall K \in \mathcal{I} \quad \Leftrightarrow \quad \exists g \in G \text{ such that } p = g \cdot q.$$

Example 2.14. The prolonged action of $\mathcal{E}_2(\mathbb{C})$ on J^2 is given by

$$g \cdot (x, y, y_x, y_{xx}) = \left(\alpha(cx + sy) + a, -sx + cy + b, \alpha \frac{cy_x - s}{sy_x + c}, \frac{\alpha y_{xx}}{(sy_x + c)^3}\right),$$

where $y_x = y^{(1)}$ and $y_{xx} = y^{(2)}$. The Euclidean curvature function[3] in (1) can be written in the coordinates of J^2 as

$$\kappa(x, y, y_x, y_{xx}) = \frac{y_{xx}}{\left(1 + y_x^2\right)^{3/2}}.$$

Though κ is not a rational differential function on J^2, the function κ^2 is. Thus κ^2 is a rational differential invariant function for the action of $\mathcal{E}_2(\mathbb{C})$. In fact one can show that κ^2 separates orbits for the prolonged action of $\mathcal{E}_2(\mathbb{C})$ on J^2. For a particular algebraic curve C defined by $F(x, y) = 0$, we can restrict κ^2 to C to obtain the map $\kappa^2|_C : C \to \mathbb{C}$ defined by

$$\frac{\left(\frac{-F_{xx}F_y^2 + 2F_{xy}F_xF_y - F_{yy}F_x^2}{F_y^3}\right)^2}{\left(1 + \left(\frac{F_x}{F_y}\right)^2\right)^3} = \frac{\left(-F_{xx}F_y^2 + 2F_{xy}F_xF_y - F_{yy}F_x^2\right)^2}{\left(F_x^2 + F_y^2\right)^3}.$$

Definition 2.15. Let an r-dimensional algebraic group G act on $\mathbb{C}^2$. A pair of rational differential invariants $\mathcal{I} = \{K_1, K_2\}$ is said to be *classifying* if K_1 separates orbits on a Zariski-open subset $U_k \subset J^k$ for some $k < r$ and $\mathcal{I}$ separates orbits on a Zariski-open subset $U_r \subset J^r$.

[3] Note that in this formulation of Euclidean curvature, κ is a *local* invariant, and a 180-degree rotation of the curve will change the sign of $\kappa(x, y, y_x, y_{xx})$. Unlike (1), κ in this case does not take into account orientation of the curve, as y is locally parameterized with respect to x. See Olver (2001, Example 4.8) for more details.

For a particular action of G, such a pair of classifying invariants always exists, and one can explicitly construct a pair by computing generators for the field of rational invariants for the prolonged action of G (Kogan et al., 2020, Thm 2.20), using algorithms such as those found in Derksen and Kemper (2015) and Hubert and Kogan (2007). It should be noted that $\mathcal{I}$ is not unique, and different choices can lead to different differential signatures.

Definition 2.16. For a pair of classifying invariants $\mathcal{I} = \{K_1, K_2\}$, an algebraic curve C is said to be *non-exceptional* if all but finitely many points on $p \in C$ satisfy

$$j^k_C(p) \in U_k, \;\; j^r_C(p) \in U_r, \;\; \text{and} \;\; \frac{\partial K_1}{\partial y^{(k)}}, \; \frac{\partial K_2}{\partial y^{(r)}} \neq 0 \text{ at } j^r_C(p),$$

where U_k, U_r are defined in Definition 2.15 for a classifying pair $\mathcal{I}$.

A generic curve of degree d where $\binom{d+2}{2} - 2 \geq r$ is non-exceptional with respect to a given classifying set (Kogan et al., 2020, Thm 2.27).

Definition 2.17. Let $\mathcal{I} = \{K_1, K_2\}$ be a pair of classifying invariants for the action of G on $\mathbb{C}^2$ and C a non-exceptional algebraic curve with respect to $\mathcal{I}$. The map $\sigma_C : C \to \mathbb{C}^2$ defined by $\sigma_C = (K_1|_C, K_2|_C)$ is the *differential signature map* for C and its image is the *differential signature* of C, denoted $\mathcal{S}_C$.

The following appears as Theorem 2.37 in Kogan et al. (2020).

Theorem 2.18. *If algebraic curves C_0, C_1 are non-exceptional with respect to a classifying set of rational differential invariants $\mathcal{I} = \{K_1, K_2\}$ under an action of G on $\mathbb{C}^2$ then*

$$C_0 \cong_G C_1 \quad \Leftrightarrow \quad \overline{\mathcal{S}_{C_0}} = \overline{\mathcal{S}_{C_1}}.$$

Since the Zariski-closure of the differential signature of an algebraic curve $\overline{\mathcal{S}_C}$ characterizes its equivalence class under G, so does the polynomial vanishing on $\mathcal{S}_C$, referred to as the *signature polynomial* of C and denoted $S_C(\kappa_1, \kappa_2)$. Thus to determine if curves C_1 and C_2 are G-equivalent we can compare signature polynomials S_{C_1} and S_{C_2}. The differential signature map also characterizes the size of the symmetry group of C under G.

Definition 2.19. The *symmetry group* of C under G is the subgroup of G defined by

$$\mathrm{Sym}(C, G) = \{g \in G \mid C = \overline{g \cdot C}\}.$$

The following follows from Lemma 2.34 and Theorem 2.38 in Kogan et al. (2020).

Theorem 2.20. *For an algebraic curve, non-exceptional with respect to $\mathcal{I} = \{K_1, K_2\}$, the symmetry group $\mathrm{Sym}(C, G)$ is of cardinality $n < \infty$ if and only if the map σ_C is generically n : 1. Furthermore $\mathrm{Sym}(C, G)$ is infinite if and only if S_C is a single point.*

Example 2.21. Consider the action of the Euclidean group $\mathcal{E}_2(\mathbb{C})$ on curves in $\mathbb{C}^2$ (defined in Definition 2.7). In Example 2.14 we saw that κ^2 is rational invariant for the prolonged action of $\mathcal{E}_2(\mathbb{C})$ on J^2. Similarly the function

$$\kappa_s^2 = \frac{\left(y_{xxx}\left(1 + y_x^2\right) - 3y_x y_{xx}^2\right)^2}{\left(1 + y_x^2\right)^6},$$

representing the square of the derivative of curvature with respect to arc length, is also a rational invariant for this action. Together the pair $\mathcal{I} = \{\kappa^2, \kappa_s^2\}$ is a classifying set of rational differential

invariants for the action of $\mathcal{E}_2(\mathbb{C})$ on curves in $\mathbb{C}^2$. Moreover, there are no $\mathcal{I}$-exceptional algebraic curves—for details see Ruddy (2019, Sec. 4.1). By Theorem 2.18, the equivalence class of an algebraic curve C under $\mathcal{E}_2(\mathbb{C})$ is completely determined by $\overline{\mathcal{S}_C}$.

Consider the two ellipses C_1 and C_2 defined by the zero sets of

$$F_1(x, y) = x^2 + y^2 + xy - 1$$
$$F_2(x, y) = x^2 + y^2 - xy - 5x + y + 6,$$

respectively. The signature maps σ_{C_1}, σ_{C_2} are rational maps on C_1, C_2 defined by

$$\sigma_{C_1}(x, y) = \left(\kappa^2|_{C_1}, \kappa_s^2|_{C_1}\right) = \left(\frac{36\,(F_1(x,y)+1)^2}{(5x^2+8xy+5y^2)^3}, \frac{2916\,(x-y)^2\,(x+y)^2\,(F_1(x,y)+1)^2}{(5x^2+8xy+5y^2)^6}\right),$$
$$\sigma_{C_2}(x, y) = \left(\kappa^2|_{C_2}, \kappa_s^2|_{C_2}\right) = \left(\frac{36\,(F_2(x,y)+1)^2}{(5x-8xy+5y^2-22x+14y+26)^3}, \frac{2916\,(x-y-2)^2\,(x+y-4)^2\,(F_2(x,y)+1)^2}{(5x-8xy+5y^2-22x+14y+26)^6}\right).$$

From the above, we see that each map σ_{C_i} has an equivalent expression modulo $\mathcal{I}_{C_i}$ where the total degrees drop by 4.[4] Both ellipses C_1 and C_2 have symmetry groups under $\mathcal{E}_2(\mathbb{C})$ of cardinality 4 (generated by a reflection and 180°-degree rotation). Thus, by Theorem 2.20, the above maps are generically $4:1$. We can directly compute the signature polynomials S_{C_1} and S_{C_2} using elimination:

$$\begin{aligned} S_{C_1}(\kappa_1, \kappa_2) &= S_{C_2}(\kappa_2, \kappa_2) \\ &= 2916\,k_1^6 - 13608\,k_1^5 + 972\,k_1^4 k_2 + 2187\,k_1^4 + 1944\,k_1^3 k_2 + 108\,k_1^2 k_2^2 + 4\,k_2^3. \end{aligned}$$

Since these two curves have the same signature polynomial, the Zariski-closure of their images are equal, i.e. $\overline{\mathcal{S}_{C_1}} = \overline{\mathcal{S}_{C_2}}$. Thus by Theorem 2.18 the two curves are $\mathcal{E}_2(\mathbb{C})$-equivalent.

Example 2.22. For the action of the equi-affine group $\mathcal{SA}_2(\mathbb{C})$ on curves in $\mathbb{C}^2$ (defined in Definition 2.9), we can again construct a differential signature map from rational differential invariants. The following pair

$$(K_1, K_2) = \left(\frac{\left(3y^{(4)}y^{(2)} - 5\left(y^{(3)}\right)^2\right)^3}{\left(y^{(2)}\right)^8}, \frac{9y^{(5)}\left(y^{(2)}\right)^2 - 45y^{(4)}y^{(3)}y^{(2)} + 40\left(y^{(3)}\right)^3}{\left(y^{(2)}\right)^4}\right)$$

forms a classifying set of rational differential invariants. Here $K_1 = \mu^3$ where μ is classical affine curvature (Guggenheimer, 1963). For details on classifying sets of rational differential invariants for $\mathcal{SA}_2(\mathbb{C})$ and other classical linear groups see Ruddy (2019, Sec. 4.1).

2.3. Joint signatures

For any integer $n \geq 1$ and G acting on $\mathbb{C}^2$ as before, there is an induced action of G on the n-fold Cartesian product $(\mathbb{C}^2)^n$ given by

$$g \cdot ((x_1, y_1), \ldots, (x_n, y_n)) = (g \cdot (x_1, y_1), \ldots, g \cdot (x_n, y_n)).$$

On one hand, the group-equivalence problem for products of curves gives us nothing new; two plane curves C_0, C_1 are G-equivalent if and only if C_0^n, C_1^n are G-equivalent under this induced action. On the other hand, it is often possible to construct classifying invariants for the induced action which involve lower-order jets than would be needed when $n = 1$. Although the number of invariants required may increase with n, the lower-order invariants are of interest in applications, as they may be more noise-resistant. Of special interest are the invariants of order zero, giving rise to the *joint signatures*,

[4] We detect this automatically with an implementation of rational function simplification from Monagan and Pearce (2006) in Macaulay2 (Grayson and Stillman, 1997).

which were introduced in Olver (2001) and studied for many of the classical groups in the smooth setting.

In this section, we study joint signatures for the Euclidean group in the algebraic setting of this paper. We define for $n \geq 2$ the regular map

$$d_n : (\mathbb{C}^2)^n \to \mathbb{C}^{n(n-1)/2}$$
$$(x_1, y_1, \ldots, x_n, y_n) \mapsto (d_{12}, d_{13}, \ldots, d_{1n}, \ldots, d_{(n-1)n}),$$

whose coordinate functions are the squared inter-point distances

$$d_{jk} = (x_j - x_k)^2 + (y_j - y_k)^2.$$

Abusing notation, we write $d_n(C)$ for the restriction of d_n to the n-fold Cartesian product C^n for any algebraic curve $C \subset \mathbb{C}^2$.

Definition 2.23. The *Euclidean joint signature* $\mathcal{J}_C = d_4(C)$ is the image of the map $C^4 \to \mathbb{C}^6$ obtained by restricting d_4.

Since d_4 is invariant under the induced action of $\mathcal{E}_2(\mathbb{C})$ on $(\mathbb{C}^2)^4$, it is clear that if two curves are $\mathcal{E}_2(\mathbb{C})$-equivalent, then they will have the same joint signature. We will show that the converse also holds.

Theorem 2.24. *Two irreducible plane curves $C_0, C_1 \subset \mathbb{C}^2$ are $\mathcal{E}_2(\mathbb{C})$-equivalent if and only if $\mathcal{J}_{C_0} = \mathcal{J}_{C_1}$.*

The hypothesis of irreducibility cannot simply be dropped—for instance, the joint signature does not distinguish an irreducible curve from its union with any number of *isotropic lines*. Here, we define an isotropic line to be any curve which is $\mathcal{E}_2(\mathbb{C})$-equivalent to the line $\{(x, y) \in \mathbb{C}^2 \mid x = iy\}$, where i is the imaginary unit. In all that follows, we let $C \subset \mathbb{C}^2$ be an irreducible affine plane curve.

We begin with nearly-matching upper and lower bounds on the dimensions of $d_n(C)$.

Proposition 2.25. *For all $n \geq 2$, we have $\dim d_n(C) \leq n$. If C is not an isotropic line, we also have $\dim d_n(C) \geq n - 1$; in particular, $2 \leq \dim d_3(C) \leq 3$, and $3 \leq \dim d_4(C) \leq 4$.*

Proof. The first statement follows easily since $\dim d_n(C) \leq \dim(C^n)$. For the second statement, note first that $d_2(C)$ is an irreducible subvariety of $\mathbb{C}^1$ and that $0 \in d_2(C)$. Thus, $d_2(C)$ will be Zariski dense in $\mathbb{C}^1$ unless 0 is the *only* point in $d_2(C)$, which is precisely the case of an isotropic line. Thus, in all other cases, $\dim d_2(C) = 1$. For larger n, consider the projection $d_n(C) \to d_{n-1}(C)$. The fibers of this map will be 1-dimensional, except once again in the case that C is an isotropic line. Hence $\dim d_n(C) \geq \dim d_{n-1}(C) + 1$. □

Our proof of Theorem 2.24 makes repeated use of the simple fact that the squared distances separate orbits of the induced $\mathcal{E}_2(\mathbb{C})$ action on *generic* 3-tuples and 4-tuples. This is the content of Proposition 2.26, which we prove with an algebraic analogue of the moving frame method. We state sufficient conditions for genericity more precisely by defining $W_n \subset (\mathbb{C}^2)^n$ to be the Zariski-open set where none of the inter-point distances vanish:

$$W_n = \{(p_1, \ldots, p_n) \in (\mathbb{C}^2)^n \mid d_{jk}(p) \neq 0 \text{ for } j < k \text{ and } j, k \in \{1, \ldots, n\}\},$$

where $W_1 = \mathbb{C}^2$ by convention. Thus, for example, we have $((0, 0), (1, i)) \notin W_2$.

Proposition 2.26. *For $n \geq 2$, the $\mathcal{E}_2(\mathbb{C})$-orbit of any $(p_1, \ldots, p_n) \in W_n$ consists of all $(q_1, \ldots, q_n) \in (\mathbb{C}^2)^n$ such that $d_n(p_1, \ldots, p_n) = d_n(q_n, \ldots, q_n)$.*

Proof. Suppose $d_n(p_1,\dots,p_n) = d_n(q_n,\dots,q_n)$. We will show that $(p_1,\dots,p_n)$ and $(q_1,\dots,q_n)$ are in the same orbit. The converse, that points in the same orbit have the same image under d_n, is easily verified.

Without loss of generality, we may assume that $p_1 = q_1 = (0,0)$ and $p_2 = q_2 = (0, y_2)$ by applying to each of the n-tuples a suitable translation and rotation. For instance, if $p_1 = (0,0)$ and $p_2 = (x_2', y_2')$, we act with the rotation

$$\frac{1}{\sqrt{x_2'^2 + y_2'^2}} \cdot \begin{pmatrix} y_2' & -x_2' \\ x_2' & y_2' \end{pmatrix},$$

and hence we also have that $y_2 = \sqrt{x_2'^2 + y_2'^2} = \sqrt{d_2} \neq 0$. For the remaining points p_k, q_k with $k \geq 3$, we write $p_k = (x_k^p, y_k^p)$ and $q_k = (x_k^q, y_k^q)$ and consider the two equations $d_{1k}(p) = d_{1k}(q)$ and $d_{2k}(p) = d_{2k}(q)$:

$$\begin{aligned} (x_k^p)^2 + (y_k^p)^2 &= (x_k^q)^2 + (y_k^q)^2 \\ (x_k^p)^2 + (y_2 - y_k^p)^2 &= (x_k^q)^2 + (y_2 - y_k^q)^2. \end{aligned}$$

Subtracting these and dividing by y_2, we obtain $y_2 - 2y_k^p = y_2 - 2y_k^q$. Hence for all k we have $y_k^p = y_k^q$, which in turn implies that $(x_k^p)^2 = (x_k^q)^2$. We are done if $x_k^p = x_k^q$ for all k; otherwise, we may choose k minimal such $x_k^p = -x_k^q \neq 0$. Reflecting about the y-axis leaves $p_1,\dots,p_{k-1}, q_1,\dots,q_{k-1}$ unchanged, but with $p_k = q_k$. Moreover, for any $j > k$, we now have

$$(x_k - x_j^p)^2 + (y_k - y_j)^2 = (x_k - x_j^q)^2 + (y_k - y_j)^2,$$

which simplifies to $-2x_k x_j^p = -2x_k x_j^q$, and hence $x_j^p = x_j^q$. □

Any two points in the same $\mathcal{E}_2(\mathbb{C})$-orbit will have conjugate stabilizer subgroups. Arguing as in the previous proof, we may characterize a generic stabilizer under the induced action.

Proposition 2.27. *For $n \geq 2$, the subgroup of $\mathcal{E}_2(\mathbb{C})$ that stabilizes $(p_1,\dots,p_n) \in W_n$ is trivial unless $p_1,\dots,p_n$ are collinear, in which case it is generated by reflection through the line $\overline{p_1 p_2}$.*

Proof. As in the previous proof, we may assume $p_1 = (0,0)$ and $p_2 = (0, y_2)$ with $y_2 \neq 0$. A short calculation shows, for g defined by parameters (a,b,c,s) as in Example 2.21, that $g \cdot (p_1, p_2) = (p_1, p_2)$ implies immediately that $a = b = 0$ (no translation), and moreover $s\, y_2 = 0$, which in turn forces $(c,s) = (\pm 1, 0)$. Thus, the stabilizer of (p_1, p_2) is generated by reflection about the y-axis. The rest of the proposition follows from considering the action on the remaining points $p_3,\dots,p_n$. □

To apply Proposition 2.26 in the case where $(p_1,\dots,p_n) \in C^n$, we must verify that the intersection $C^n \cap W_n$ is nonempty. This turns out to be true for all irreducible C except for the isotropic lines.

Lemma 2.28. *Suppose $C \subset \mathbb{C}^2$ is an irreducible algebraic curve which is not an isotropic line. For any fixed $n \geq 1$, the intersection $C^n \cap W_n$ is nonempty. In fact, for any fixed $(p_1,\dots,p_{n-1}) \in C^{n-1} \cap W_{n-1}$, we have $(p_1,\dots,p_n) \in C^n \cap W_n$ for generic $p_n \in C$.*

Proof. The claim is vacuous for $n = 1$. For larger n, fix $(p_1,\dots,p_{n-1}) \in C^{n-1} \cap W_{n-1}$ and consider the Zariski open sets $U_1,\dots,U_{n-1} \subset C$ defined by $U_i = \{p \in C \mid d(p_i, p) \neq 0\}$. If any of the sets $C \cap U_i$ were empty, then C would be contained in the union of two isotropic lines, namely

$$\{(x,y) \in \mathbb{C}^2 \mid ((x - x_i) + i(y - y_i))\,((x - x_i) - i(y - y_i)) = 0\}.$$

Since C is irreducible, this would imply that C is one of these lines; thus $C \cap U_i \neq \emptyset$ for each $i = 1,\dots,n-1$. This gives us that $(p_1,\dots,p_n) \in C^n \cap W_n$ for all $p_n \in C \cap U_1 \cap \cdots \cap U_{n-1} \neq \emptyset$. □

To prove Theorem 2.24, we align two curves with the same joint signature by applying the moving frame method to suitably generic triples of points, and then conclude that the aligned curves are equal by applying the following lemma.

Lemma 2.29. *Let $C_0, C_1 \subset \mathbb{C}^2$ be irreducible algebraic curves which are not isotropic lines. For $n \geq 3$, suppose there exists $(p_1, \dots, p_{n-1}) \in C_0^{n-1} \cap C_1^{n-1}$ such that*

$$d_n(p_1 \times \cdots \times p_{n-1} \times C_0) = d_n(p_1 \times \cdots \times p_{n-1} \times C_1).$$

Then C_0 and C_1 are $\mathcal{E}_2(\mathbb{C})$-equivalent.

Proof. Pick $p_n \in C_0$ satisfying the genericity conditions of Lemma 2.28; by assumption, there exists $p_n' \in C_1$ with $d(p_1, \dots, p_n) = d(p_1, \dots, p_n')$. By Proposition 2.26, we have that $(p_1, \dots, p_n) = g \cdot (p_1, \dots, p_n')$ for some $g \in \mathcal{E}_2(\mathbb{C})$. This implies that g stabilizes $(p_1, \dots, p_{n-1})$, so by Proposition 2.27 it follows that g is either the identity or a reflection about the line $\overline{p_1 p_2}$. Thus, C_0 and gC_1 intersect in infinitely many points, and we may conclude that $C_0 = gC_1$. □

Proof of Theorem 2.24. Let $\mathcal{J}$ be the joint signature of irreducible curves C_1 and C_2. Without loss of generality, assume that neither curve is an isotropic line, in which case the statement is trivial. Fix generic $p_1, p_2, p_3 \in C_1$. By Proposition 2.26, we may assume $p_1, p_2, p_3 \in C_2$ by acting on C_2 with an appropriate $\mathcal{E}_2(\mathbb{C})$ element. Let $\mathcal{J}'$ be the intersection of $\mathcal{J}$ with the coordinate hyperplanes $d_{ij} = d(p_i, p_j)$ for $1 \leq i < j \leq 3$. Although $\dim \mathcal{J}$ may be either 3 or 4, the genericity of $p_1, \dots, p_3$ implies that $\mathcal{J}'$ is a curve in either case, by an argument analogous to that given in Proposition 2.25. Indeed, the image of the map $C \ni p_4 \mapsto (p_1, \dots, p_4) \in \mathcal{J}'$ is an irreducible variety of dimension at most 1, which contains two distinct points since C is not an isotropic line. Thus the image has dimension 1, implying the same for $\mathcal{J}'$.

Now, for generic $p_4 \in C_1$, we have that $d_4(p_1, p_2, p_3, p_4)$ is a smooth point on $\mathcal{J}'$. Fixing generic p_4, there exists $p_4' \in C_2$ with $d_4(p_1, p_2, p_3, p_4) = d_4(p_1, p_2, p_3, p_4')$. Thus, the irreducible curves $d_4(p_1 \times p_2 \times p_3 \times C_1)$ and $d_4(p_1 \times p_2 \times p_3 \times C_2)$ intersect in a smooth point. We conclude $d_4(p_1 \times p_2 \times p_3 \times C_1) = d_4(p_1 \times p_2 \times p_3 \times C_2)$, and hence $C_0 \cong_{\mathcal{E}_2(\mathbb{C})} C_1$ by Lemma 2.29. □

We now state and prove the analogue of Theorem 2.20 for joint signatures.

Lemma 2.30. *Let C be an irreducible algebraic curve. The group of Euclidean symmetries of C has the same cardinality as the fiber over a generic point in its joint signature: that is, for generic $p_1, \dots, p_4 \in C$,*

$$\left|d_{4|_C}^{-1}(d_4(p_1, p_2, p_3, p_4))\right| = |Sym(C, \mathcal{E}_2(\mathbb{C}))|.$$

Proof. Once again we may assume C is not an isotropic line so that there exists $(p_1, \dots, p_4) \in C^4 \cap W_4$. By Proposition 2.26, the fiber $d_4^{-1}(d_4(p_1, p_2, p_3, p_4))$ is exactly the orbit of (p_1, p_2, p_3, p_4) under $\mathcal{E}_2(\mathbb{C})$. First suppose that C is a (non-isotropic) line. Then there is a translational subgroup of $\mathcal{E}_2(\mathbb{C})$ along the line, also a subgroup of $\mathrm{Sym}(C, \mathcal{E}_2(\mathbb{C}))$, which preserves the distances between the 4-tuple of points as they move along the curve. Thus the fiber and symmetry group are both infinite.

For C of degree greater than 2, a generic 4-tuple of points is non-collinear and has trivial stabilizer under $\mathcal{E}_2(\mathbb{C})$ by Proposition 2.27. Thus each element of $\mathrm{Sym}(C, \mathcal{E}_2(\mathbb{C}))$ sends (p_1, p_2, p_3, p_4) to a distinct 4-tuple in the fiber, implying that

$$\left|d_{4|_C}^{-1}(d_4(p_1, p_2, p_3, p_4))\right| \geq |\mathrm{Sym}(C, \mathcal{E}_2(\mathbb{C}))|.$$

Now fix $(q_1, \dots, q_4) \in d_{4|_C}^{-1}(d_4(p_1, p_2, p_3, p_4))$, so that there exists a $g \in \mathcal{E}_2(\mathbb{C})$ such that $g \cdot (p_1, p_2, p_3, p_4) = (q_1, q_2, q_3, q_4)$; note, moreover, that distinct points in the fiber produce distinct group elements. Consider the curve $C' = g \cdot C$. Clearly C' has the same joint signature as C, and hence we satisfy the hypothesis of Theorem 2.24. Thus the proof of Theorem 2.24 implies that

$$d_4(p_1 \times p_2 \times p_3 \times C) = d_4(p_1 \times p_2 \times p_3 \times C').$$

Finally the proof of Lemma 2.29 implies that C and C' must be related by either the identity element of $\mathcal{E}_2(\mathbb{C})$ or a reflection. However, since (p_1, p_2, p_3, p_4) are non-collinear, the stabilizer is non-trivial and $C = C'$. Thus each element of the fiber gives rise to a unique element of $\mathrm{Sym}(C, \mathcal{E}_2(\mathbb{C}))$ implying that

$$|d_{4|C}^{-1}(d_4(p_1, p_2, p_3, p_4))| \leq |\mathrm{Sym}(C, \mathcal{E}_2(\mathbb{C}))|,$$

proving the lemma. □

Proposition 2.31. *For an irreducible algebraic curve C different from an isotropic line, the following are equivalent.*

(1) $\dim(\mathcal{J}_C) = 4$.
(2) The symmetry group $|Sym(C, \mathcal{E}_2(\mathbb{C}))| = n < \infty$.
(3) The map d_4 *is generically* $n : 1$.

Proof. Lemma 2.30 immediately implies that statements (2) and (3) are equivalent. The dimension of the joint signature is four (the dimension of C^4) if and only if a generic fiber of the map is of finite cardinality (see e.g. Shafarevich, 1994, Ch. 1, Sec. 6.3, Thm 1.25), and hence statements (1) and (2) are equivalent. □

The next proposition immediately follows by Proposition 2.25.

Proposition 2.32. *For an irreducible algebraic curve C different from an isotropic line,* $\dim(\mathcal{J}_C) = 3$ *if and only if the symmetry group* $Sym(C, \mathcal{E}_2(\mathbb{C}))$ *is infinite.*

As in the case of differential signature, the dimension of the joint signature drops when the curve has an infinite symmetry group under $\mathcal{E}_2(\mathbb{C})$. In the event the symmetry group is finite, the size of this subgroup is exactly the size of a generic fiber of the joint signature map.

Example 2.33. A classical result from differential geometry states that the only smooth plane curves of constant curvature are circles and lines. This is mirrored by the fact that the joint signatures of these curves have dimension 3 instead of 4; equivalently, by Proposition 2.25, the image of the map $d_{3|C}$ is a surface in $\mathbb{C}^3$. When C is a non-isotropic line, the equation of this surface is

$$d_{12}^2 - 2\,d_{12}d_{13} + d_{13}^2 - 2\,d_{12}d_{23} - 2\,d_{13}d_{23} + d_{23}^2 = 0$$

and when C is a unit circle, it is given by the *Heron polynomial*

$$d_{12}d_{13}d_{23} + d_{12}^2 - 2\,d_{12}d_{13} + d_{13}^2 - 2\,d_{12}d_{23} - 2\,d_{13}d_{23} + d_{23}^2 = 0.$$

We end this section with a discussion about joint signatures for other algebraic group actions. In Olver (2001), the author presents a *smooth* characterization of joint invariants for many of these groups over $\mathbb{R}$. For instance, consider the action of $\mathcal{SA}_2(\mathbb{R})$ on n-tuples of $\mathbb{R}^2$. The fundamental joint invariant is given by the signed area functions $v(i, j, k)$ for $1 \leq i < j < k \leq n$ (Olver, 2001, Thm 3.3) where

$$v(i, j, k) = x_i(y_j - y_k) - x_j(y_i - y_k) + x_k(y_i - y_j).$$

Though the number of such invariants increases in size rapidly as n grows, there exist many linear syzygies between these functions. In particular the invariants $v(1, 2, k)$, $v(1, 3, k)$ for $k = 2, \ldots, n$ generate the other invariants (Olver, 2001, Thm 8.8). Thus for curves under $\mathcal{SA}_2(\mathbb{C})$ we can define the map $v_6 : (\mathbb{C}^2)^6 \to \mathbb{C}^7$ by

$$(x_1, y_1, \ldots, x_6, y_6)$$
$$\mapsto (v(1,2,3), v(1,2,4), v(1,2,5), v(1,2,6), v(1,3,4), v(1,3,5), v(1,3,6)). \tag{3}$$

Mirroring the construction for real curves under $\mathcal{SA}_2(\mathbb{R})$ in Olver (2001, Ex. 8.6), we can define the **equi-affine joint signature** of a curve C to be $\mathcal{J}_C^{\mathcal{SA}} = v_6(C^6)$. Though there are fundamental invariants for n as low as 3, it is necessary to consider 6-tuples of points on curves since all curves have the same image under the map v_n (defined as above) when $n < 6$. For other groups, the fundamental joint invariants presented in Olver (2001) similarly yield sets of algebraic invariants. It would be interesting to construct general conditions for sets of joint invariants to characterize orbits of curves.

Remark 2.34. While we conduct experiments in Section 4 comparing the equi-affine joint signature to the equi-affine differential signature, we do not explicitly prove that $\mathcal{J}_C^{\mathcal{SA}}$ characterizes orbits of curves under $\mathcal{SA}_2(\mathbb{C})$, as we do for the Euclidean joint signature. However, as the seven area invariants defining v_6 generate the other fundamental area invariants through linear relations, it is likely that they separate orbits and that one can prove this characterization using an argument similar to that in this section.

3. Witness sets for signatures

3.1. Background

A comprehensive overview of numerical algebraic geometry may be found in the survey (Sommese et al., 2005) or books (Wampler et al., 2005; Bates et al., 2013). Here we develop the notions that we need, illustrated by several examples related to the previous section.

The main data structures in numerical algebraic geometry are variations on the notion of a *witness set*. The overarching idea is to represent an irreducible variety $Y \subset \mathbb{C}^n$ by its intersection with a generic affine linear subspace of complementary dimension. The number of points in such an intersection is the degree $\deg Y$, which may be understood as the degree of the projective closure of Y under the usual embedding $\mathbb{C}^m \ni (x_1, \ldots, x_m) \mapsto [x_1 : \cdots : x_m : 1] \in \mathbb{P}(\mathbb{C}^{m+1})$. We define a c-slice in $\mathbb{C}^m$ to be a polynomial system consisting of c affine hyperplanes, $L = (l_1, \ldots, l_c)$ with $l_i \in \mathbb{C}[x_1, \ldots, x_m]_{\leq 1}$. For convenience we write L or L^c in place of its vanishing locus $V(L(x))$, an affine linear space of codimension c. For Y an irreducible variety of dimension d and a generic slice L^d, the intersection $Y \cap L^d$ is *transverse*, consisting of $\deg Y$ isolated, nonsingular points.

The notion of a *pseudo-witness set*, first appearing in Hauenstein and Sommese (2010), allows us to represent the closed image of a rational map $Y = \overline{\operatorname{im} \Phi}$ without knowing its implicit defining equations. Our Definition 3.1 differs slightly from that used in the standard references (Hauenstein and Sommese, 2010, 2013; Bates et al., 2013); to distinguish our setup, we provisionally use the term *weak pseudowitness set*.

Definition 3.1. Let $f = (f_1, \ldots, f_N)$ so that $V(f) \subset \mathbb{C}^n$ is Zariski-closed, $X \subset V(f)$ be one of its irreducible components, and $\Phi : X \dashrightarrow \mathbb{C}^m$ be a rational map. Set $c = \operatorname{codim} V(f)$, $d = \dim \overline{\operatorname{im} \Phi}$. A weak pseudowitness set for Φ is a quadruple $\left(f, \Phi, (L|L'), \{w_1, \ldots, w_e\}\right)$, where L is a generic affine d-slice of $\overline{\operatorname{im} \Phi}$, L' is a generic affine $(n-c-d)$-slice of X, and such that $w_1, \ldots, w_e$ are points in $X \cap L'$ where $\Phi(w_1), \ldots, \Phi(w_e)$ are all defined and such that $\overline{\operatorname{im} \Phi} \cap L = \{\Phi(w_1), \ldots, \Phi(w_e)\}$ and $e = \deg \overline{\operatorname{im} \Phi}$.

For all examples considered in our paper, the map Φ will have generically finite fibers, so that $n - c = d$. In particular, for the differential signatures we will always have $(n, c, d, m) = (2, 1, 1, 2)$, whereas for the joint signatures we have $(n, c, d, m) = (8, 4, 4, 6)$. Consequently, the linear space L' does not play a role in our experiments; nevertheless, we consider it in Algorithm 1 for the sake of full generality.

Example 3.2. Consider again the ellipses from Example 2.21. We represent $Y = \overline{\operatorname{im} \sigma_{C_1}} = \overline{\operatorname{im} \sigma_{C_2}}$ not by the signature polynomial, but rather by its intersection with a generic slice in the codomain:

$L^1 = \{l_1 x + l_2 y + l_3 = 0\}$. For the particular choice of $(l_1, l_2, l_3) = (1, -2, 1)$, we have that $\overline{\operatorname{im} \sigma_{C_i}} \cap L^1$ consists of 6 points $(x_i, y_i) \in \mathbb{C}^2$:

x_i	y_i
$-.120636 - .0158199\,i$	$.439682 - .00790993\,i$
$-.120636 + .0158199\,i$	$.439682 + .00790993\,i$
$.0305676 - .0677494\,i$	$.515284 - .0338747\,i$
$.0305676 + .0677494\,i$	$.515284 + .0338747\,i$
.501814	.750907
4.17832	2.58916

Compared to the more standard definition of a witness set, in Definition 3.1 we allow that the containment $\{w_1, \ldots, w_e\} \subset L' \cap \Phi^{-1}\left(\overline{\operatorname{im} \Phi} \cap L\right)$ may be proper. When Φ is the signature of a curve with many symmetries, this may be preferable, since fewer points need to be stored due to Theorem 2.20 and Proposition 2.31. The data in Definition 3.1 are already sufficient for testing queries of the form $y \in \overline{\operatorname{im} \Phi}$, as noted in Hauenstein and Sommese (2010, Remark 2). For testing, $y \in \operatorname{im} \Phi$ and other applications, the stronger notion is required (Hauenstein and Sommese, 2013). Further applications of pseudowitness sets may be found in the references (Chen and Kileel, 2019; Brysiewicz, 2018; Hauenstein and Regan, 2020; Hauenstein and Sottile, 2014).

In our context, equations defining $\overline{\operatorname{im} \Phi}$ are seldom known, so in what follows we may informally refer to the objects of Definition 3.1 and their multiprojective counterparts in Definition 3.3 as "witness sets" without ambiguity. In practice, we can at best hope that our numerical approximations to points $\Phi(w_1), \ldots, \Phi(w_e)$ lie sufficiently close to $\overline{\operatorname{im} \Phi} \cap L$: to clearly distinguish practice from theory, we occasionally use the term *numerical (weak / pseudo) witness set.*

Following Hauenstein and Rodriguez (2020), Leykin et al. (2018), Hauenstein et al. (2022), we give a multiprojective generalization of Definition 3.1. For irreducible $Y \subset \mathbb{C}^m$, we fix $(m_1, \ldots, m_k)$, an integer partition of m, and consider Y in the affine space $\mathbb{C}^{m_1} \times \cdots \times \mathbb{C}^{m_k}$. We consider slices $L^{\boldsymbol{e}} = L^{e_1} | \cdots | L^{e_k}$, where $\boldsymbol{e} = (e_1, \ldots, e_k) \in \mathbb{N}^k$ is an integral vector such that $e_1 + \cdots + e_k = \dim Y$, and L^{e_j} is a e_j-slice consisting of e_j affine hyperplanes in the coordinates of $\mathbb{C}^{m_j}$. We say that $\boldsymbol{e}$ is a *multidimension* of Y if for generic $L^{\boldsymbol{e}}$ the intersection $Y \cap L^{\boldsymbol{e}}$ is a finite set of nonsingular points; the number of points for such $L^{\boldsymbol{e}}$ is a constant called the $\boldsymbol{e}$*-multidegree* $\deg_{\boldsymbol{e}} Y$. These definitions reflect the geometry of the *multiprojective closure* of X under the embedding

$$\begin{aligned} &Y \ni (y_1, \ldots, y_m) \\ &\mapsto \left([y_1 : \cdots : y_{m_1} : 1], \ldots, [y_{m-m_k+1} : \cdots : y_m : 1]\right) \in \mathbb{P}(\mathbb{C}^{m_1+1}) \times \cdots \times \mathbb{P}(\mathbb{C}^{m_k+1}). \end{aligned}$$

Definition 3.3. Let f, X, c, L', Φ be as in 3.1, and $\boldsymbol{e}$ be a multi-dimension of $\overline{\operatorname{im} \Phi}$ corresponding to some partition of n. An $\boldsymbol{e}$-weak pseudowitness set for Φ consists of $\left(f, \Phi, (L^{\boldsymbol{e}} | L'), \{w_1, \ldots, w_e\}\right)$, such that $\overline{\operatorname{im} \Phi} \cap L^{\boldsymbol{e}} = \{\Phi(w_1), \ldots, \Phi(w_e)\}$ and $e = \deg_{\boldsymbol{e}} \overline{\operatorname{im} \Phi}$.

Example 3.4. Continuing as in Example 3.2, we now consider coordinate slices in the codomain of σ_{C_i} of the form $L^{(1,0)} = \{l_1 x + l_2 = 0\}$. Specializing to the generic slice $(l_1, l_2) = (3, 1)$ yields now 3 points:

x_i	y_i
$-.333333$	$1.53234 + 1.11277\,i$
$-.333333$	$1.53234 - 1.11277\,i$
$-.333333$	-6.06468

The general membership test for multiprojective varieties proposed in Hauenstein and Rodriguez (2020) uses the stronger notion of a witness collection. This is required since for an arbitrary point $y \in Y$ there may not exist transverse slices $L^{\boldsymbol{e}} \ni y$ for $\boldsymbol{e}$ ranging over all multidimensions of Y—see Hauenstein and Rodriguez (2020, Example 3.1). This subtlety is not encountered for generic $y \in Y$; we record this basic fact in Proposition 3.5.

Proposition 3.5. *Fix irreducible $Y \subset \mathbb{C}^{m_1} \times \cdots \times \mathbb{C}^{m_k}$ and $\boldsymbol{e}$ some multi-dimension of Y. For $y = (y_1, \cdots, y_k) \in Y$ generic, there exists an $\boldsymbol{e}$-slice $L^{\boldsymbol{e}} \ni y$ such that $\dim(Y \cap L^{\boldsymbol{e}}) = 0$. Moreover, for $y \notin Y_{sing}$, we also have that $y \notin (Y \cap L^{\boldsymbol{e}})_{sing}$ for generic $L^{\boldsymbol{e}}$.*

Proof. For generic y_1 in the image of $\pi_1 : Y \to \mathbb{C}^{m_1}$ we have that the fiber $\pi_1^{-1}(x_1)$ has dimension $\dim Y - \dim \pi_1(Y)$. Choose such an y_1 and let $L^{e_1} \ni y_1$ be generic so that $\pi_1(Y) \cap L^{e_1}$ has dimension $\dim \pi_1(Y) - e_1$. It follows that $Y \cap L^{e_1}$ has dimension $\dim Y - e_1$. This construction holds for all y_1 on some Zariski open $U_1 \subset \pi_1(Y)$. Repeating this construction for the remaining factors yields $U_2, \ldots, U_k$ such that the first part holds for all $y \in U_1 \times \cdots \times U_k$. The second part follows from Bertini's theorems, e.g. Harris (2013, Thm 17.16). □

3.2. A general equality test

Now let $\Phi_0 : X_0 \dashrightarrow \mathbb{C}^m$ and $\Phi_1 : X_1 \dashrightarrow \mathbb{C}^m$ denote two rational maps with each $X_i \subset \mathbb{C}^{n_i}$ of codimension c_i. Problem 2 from the introduction asks us to decide whether or not their images are equal up to Zariski closure. We describe a probabilistic procedure (Algorithm 1) which refines the general membership and equality tests from numerical algebraic geometry, which are summarized in Wampler et al. (2005, Ch. 13, 15) and (Bates et al., 2013, Ch. 8, 16). As noted in the Introduction, our setup is motivated by an efficient solution to Problem 1. Following the standard terminology, our test correctly decides equality with "probability-one" in an idealized model of computation. This is the content of Theorem 3.6. Standard disclaimers apply, since any implementation must rely on numerical approximations in floating-point. A thorough discussion of these issues may be found in Bates et al. (2013, Ch. 3, pp. 43–45).

Algorithm 1 assumes different representations for the two maps. The map Φ_1 is represented by a witness set in the sense of Definition 3.1, say $(f_1, \Phi_1, (L_1 | L_1'), \{w_1, \ldots, w_e\})$. In fact, the only data needed by Algorithm 1 are the map itself Φ_1, the slice L_1, and the points $w_1, \ldots, w_e$. For the map Φ_0, we need only a sampling oracle that produces generic points on X_0 and $c_0 = \operatorname{codim}(X_0)$-many reduced equations vanishing on X_0.

Suppose $\dim \overline{\operatorname{im} \Phi_0} = \dim \overline{\operatorname{im} \Phi_1} = d$. There is a probabilistic membership test for queries of the form $\Phi_0(x_0) \in \overline{\operatorname{im} \Phi_1}$ based on homotopy continuation. The relevant homotopy depends parametrically on L_1, a d-slice $L_0 \ni \Phi_0(x_0)$, a $(n - c_0 - d)$-slice $L_0' \ni x_0$, and a regular sequence $f_0 = (f_{0,1}, \ldots, f_{0,c_0})$ which is generically reduced with respect to X_0. The homotopy H is defined by setting

$$H(x; t) = \begin{pmatrix} f_0(x) \\ L_0'(x) \\ t\, L_1 \circ \Phi_0 + (1 - t)\, L_0 \circ \Phi_0(x) \end{pmatrix} = 0. \tag{4}$$

In simple terms, H moves a slice through $\Phi_0(x_0)$ to the slice witnessing $\overline{\operatorname{im} \Phi_1}$ as t goes from 0 to 1. A solution curve associated to (4) is a smooth map $x : [0, 1] \to \mathbb{C}^n$ such that $H(x(t), t) = 0$ for all t. For generic parameters L_0, L_1, L_0' the Jacobian $H_x(x, t)$ is invertible for all $t \in [0, 1]$, solution curves satisfy the ODE

$$x'(t) = -H_x(x, t)^{-1} H_t(x, t),$$

and each of the points $w_1, \ldots, w_e$ is the endpoint of some solution curve x with $x(0) \in X \cap L_0'$. These statements follow from more general results on *coefficient-parameter homotopy*, as presented in Morgan and Sommese (1989) or Wampler et al. (2005, Thm 7.1.1). We assume a subroutine TRACK(H, x_0) which returns $x(1)$ for the solution curve based at x_0. In practice, the curve $x(t)$ is approximated by numerical predictor/corrector methods (Allgower and Georg, 1990; Morgan, 2009). We allow our TRACK routine to fail; this will occur, for instance, when $\Phi_0(x_0)$ is a singular point on $\overline{\operatorname{im} \Phi_0}$. However, it will succeed for generic (and hence *almost all*) choices of parameters and $x_0 \in \mathbb{C}^{n_0}$.

Theorem 3.6. *For generic x_0, L_0, L_0', L_1, Algorithm 1 correctly decides if $\overline{\operatorname{im} \Phi_0} = \overline{\operatorname{im} \Phi_1}$.*

Algorithm 1. Probability-1 equality test.

Input: Let $X_0 \subset \mathbb{C}^{n_0}, X_1 \subset \mathbb{C}^{n_1}$ be irreducible algebraic varieties, and $\Phi_0 : X_0 \to \mathbb{C}^m$, $\Phi_1 : X_1 \to \mathbb{C}^m$ be rational maps, represented via the following ingredients:

1) $(L_1, \{w_1, \ldots, w_e\})$ with $\overline{\operatorname{im}\Phi_1} \cap L_1 = \{\Phi_1(w_1), \ldots, \Phi_e(w_e)\}$ and $e = \deg \overline{\operatorname{im}\Phi_1}$ (cf. Definition 3.1),
2) $f_{0,1}, \ldots, f_{0,c_0} \in \mathbb{C}[x_1, \ldots, x_{n_0}]$: a generically reduced regular sequence such that $\operatorname{codim}(X_0) = c_0$ and $X_0 \subset V(f_1, \ldots, f_{c_0})$,
3) an oracle for sampling a point $x_0 \in X_0$, and
4) explicit rational functions representing each map Φ_i.

Output: YES if $\overline{\operatorname{im}\Phi_0} = \overline{\operatorname{im}\Phi_1}$ and NO if $\overline{\operatorname{im}\Phi_0} \neq \overline{\operatorname{im}\Phi_1}$.

1: sample $x_0 \in X_0$
2: $T_{x_0}(f) \leftarrow \ker(D f)_{x_0}$
3: $d \leftarrow \operatorname{rank}(D\Phi_0)_{x_0}|_{T_{x_0}(f)}$
4: **if** $d \neq \dim \overline{\operatorname{im}\Phi_1}$ **then return** NO
5: $H(x;t) \leftarrow$ the homotopy from equation (4) (L_0 generic)
6: $x_1 \leftarrow \text{TRACK}(H, x_0)$
7: **if** $\Phi_0(x_1) \in \{\Phi_1(w_1), \ldots, \Phi_1(w_e)\}$ **return** YES
else return NO

Fig. 2. A general, probabilistic equality test for rational maps.

Remark 3.7. The set of "non-generic" slices in this theorem is dependent on the maps Φ_0 and Φ_1. In practice, an oracle for sampling generic points could be provided by either a parametrization or by homotopy continuation using known equations for X_0. The dimension $\dim \overline{\operatorname{im}\Phi_1}$ is implicit in the description of the witness set.

Proof. Since x_0 is generic and f_0 is generically reduced, we may assume that $d = \dim \overline{\operatorname{im}\Phi_0}$. Noting line 4, we are done unless $d = \dim \overline{\operatorname{im}\Phi_1}$. In this case, since the $\overline{\operatorname{im}\Phi_i}$ are irreducible,

$$\dim\left(\overline{\operatorname{im}\Phi_0} \cap \overline{\operatorname{im}\Phi_1}\right) = d \quad \Leftrightarrow \quad \overline{\operatorname{im}\Phi_0} = \overline{\operatorname{im}\Phi_1}. \tag{5}$$

As previously mentioned, generic slices give that the solution curve $x(t)$ associated to (4) with initial value x_0 exists and satisfies $x(t) \in V(f) \setminus V(f)_{\text{sing}}$ for all $t \in [0, 1]$. The endpoint x_1 is, *a priori*, a point of $V(f)$. Since $X_0 \setminus (X_0)_{\text{sing}}$ is a connected component of $V(f) \setminus V(f)_{\text{sing}}$ in the complex topology and $x_0 \in X_0$, so also must $x_1 \in X_0$. Hence $\Phi_0(x_1) \in \overline{\operatorname{im}\Phi_0} \cap L_1$. Now if $\overline{\operatorname{im}\Phi_0} = \overline{\operatorname{im}\Phi_1}$, then clearly we must have

$$\Phi_0(x_1) \in \overline{\operatorname{im}\Phi_1} \cap L_1 = \{\Phi_1(w_1), \ldots, \Phi_1(w_e)\}, \tag{6}$$

as is tested on line 7. Conversely, if (6) holds, then

$$\dim(\overline{\operatorname{im}\Phi_0} \cap \overline{\operatorname{im}\Phi_1} \cap L_1) \geq 0,$$

which by (5) and the genericity of L_1 implies $\overline{\operatorname{im}\Phi_0} = \overline{\operatorname{im}\Phi_1}$. □

In the multiprojective setting, we may give a similar argument. The only added subtlety is that extra genericity may be needed so that the Jacobian $H_x(x_0, 0)$ is invertible. This follows from Proposition 3.5.

3.3. Witness sets for signatures

Our implementation of Algorithm 1 treats only the special case where the domain of each rational map is some Cartesian product of irreducible plane curves, say $X_i = C_i^k$ for some integer k. For the purpose of our implementation, the various ingredients for the input to Algorithm 1 are easily provided. Suppose $\mathcal{I}_{C_i} = \langle f_i \rangle$ for $i = 0, 1$. The reduced regular sequence we need is simply $(f_0(x_1, y_1), \ldots, f_0(x_k, y_k))$. Sampling from X_0 amounts to sampling k times from C_0; we sample the curve C_0 using homotopy continuation from a linear-product start system (Wampler et al., 2005, Sec. 8.4.3).

It remains to discuss computation of the witness set for the image of the signature map. To do this, we compute solutions to parametric systems of equations

$$f(x_1, y_1; p) = \cdots = f(x_k, y_k; p) = \ell_1(\Phi(x, y; p)) = \cdots = \ell_k(\Phi(x, y; p)) = 0, \tag{7}$$

where we allow both the parameters defining the curve p and the parameters defining the slice $L = (\ell_1, \ldots, \ell_k)$ to vary. For instance, a parametric *generic plane curve* of degree d has the form

$$f(x, y; p) = p_{0,0} + p_{1,0}x + p_{0,1}y + p_{1,1}xy + \cdots + p_{0,d}y^d.$$

For differential signatures we have $k = 1$, and we could simply write $\Phi(x_1, y_1; p)$, whereas for joint signatures we have $k = 4$ and could write $\Phi(x_1, \ldots, x_4, y_1, \ldots, y_4)$.

Let us now write Ψ_p for the (differential or joint) signature map restricted to the curve defined by particular parameter values p. When p is generic, $\overline{\operatorname{im}\Phi_p}$ of this curve has dimension k; thus, by generic smoothness, it follows for generic slice $L = (\ell_1, \ldots, \ell_k)$ there will be finitely many reduced points in $\overline{\operatorname{im}\Phi_p} \cap L$. Moreover, genericity of p implies that the map $(x, y) \mapsto \Phi(x, y; p)$ is generically finite-to-one. Associated to the system (7) is an incidence correspondence

$$V_\Phi = \{(x_1, y_1, \ldots, x_k, y_k, p, L) \in (\mathbb{C}^2)^k \times \mathbb{C}^{\binom{d+2}{2}} \times \mathbb{G}_{k,m} \mid f(x_i, y_i, p) = 0, \Phi(x, y; p) \in L\},$$

where $\mathbb{G}_{k,m}$ denotes the Grassmannian of codimension-k affine subspaces of $\mathbb{C}^m$. We recall that this incidence variety V_Φ has a unique irreducible component which projects dominantly on the space of unknowns $(\mathbb{C}^2)^k$, referred to as the *dominant component* (Duff et al., 2019, Remark 2.2). We take a Zariski-open set $U \subset (\mathbb{C}^2)^k$ such that for any fixed $(x, y) \in U$, the set of solutions to the linear equations $f(x_1, y_1; p) = \cdots = f(x_k, y_k; p)$ (7) in the parameters (p, L) has the maximal codimension k. Letting $U' \subset (\mathbb{C}^2)^k \times \mathbb{C}^{\binom{d+2}{2}} \times \mathbb{G}_{k,m}$ denote the preimage of U under coordinate projection, the dominant component $\widehat{V_\Phi}$ may be defined as the Zariski closure of U'.

The construction of the dominant component described above holds for other linear systems of curves. We often have that $V_\Phi = \widehat{V_\Phi}$, since V_Φ can be expressed as the graph of a rational map between affine spaces; for instance, in the case of the joint signatures of generic curves, we have $k = 4$ and may express certain parameters as rational functions in (x, y) and the other parameters by solving linear equations in p:

$$\begin{aligned}
p_{0,0} &= -(x_2 p_{1,0} + y_2 p_{0,1} + \cdots) \\
p_{1,0} &= (x_1 - x_2)^{-1} \left((y_1 - y_2)\, p_{0,1} + \left(x_1^2 - x_2^2\right) p_{2,0} + \cdots \right) \\
p_{0,1} &= \cdots \\
p_{1,1} &= \cdots
\end{aligned}$$

For other families of curves, we caution that there might well be additional components of V_Φ when the general member of the system is reducible, as is the case for the family of curves

$$f(x, y; p) = x(p_1 x^2 + p_2 y + c + p_3 x + p_4 y^2 + p_5).$$

The incidence variety $\{(x_1, \ldots, x_4, y_1, \ldots, y_4, p) \mid f(x_1, y_1; p) = \cdots = f(x_4, y_k; p) = 0\}$ has 16 irreducible components, each uniquely determined by the vanishing of some subset of $\{x_1, x_2, x_3, x_4\}$. The dominant component of V_Φ corresponds to the empty subset: its degree as a branched cover over $\mathbb{C}^5 \times \mathbb{G}_{4,6}$ is 168, and the generic fiber gives a pseudowitness set for the conic $p_1 x^2 + p_2 y + c + p_3 x + p_4 y^2 + p_5$. For this example, we may take U to be the set of 4-tuples of points $(x_1, y_1), \ldots, (x_4, y_4)$ which impose independent condition on conics and such that $x_i \neq 0$ for all i.

In general, the projection $\pi : \widehat{V_\Phi} \to \mathbb{C}^{\binom{d+2}{2}} \times \mathbb{G}_{k,m}$ is a branched cover of irreducible varieties, and thus, for generic (p, L), the associated monodromy group acts transitively on the fiber $\pi^{-1}(p, L)$. The fiber gives a pseudowitness set for $\overline{\operatorname{im}\Phi_p}$. Let N denote the degree of the branched cover π (i.e. $N = d(d-1)$ for differential signatures, and $N = 12d(d^3 - 1)$ for joint signatures), so that the monodromy

group $\mathcal{M}(\Phi; p, L)$ may be viewed as a subgroup of the symmetric group S_N. For differential and joint signatures of generic degree-d curves, these monodromy groups are full symmetric for $d \geq 2$. For more structured families of curves, or the multiprojective witness sets considered in our experiments, the corresponding monodromy group will be a subgroup of the wreath product $S_{N_1} \wr S_{N_2}$, where N_1 is the size of the generic symmetry group and $N_2 = \deg \overline{\operatorname{im} \Phi_p}$. The monodromy group is said to be *imprimitive*; for $N_1 > 1$, the *decomposable monodromy* technique from Améndola et al. (2021) may be used to speed up witness set computation.

Example 3.8. Consider the family of quadrifolia, or rose curves, given by

$$f(x, y) = (x^2 + y^2)^3 - px^2y^2 = 0.$$

The symmetry group for generic p is the dihedral group D_8, and thus the joint signature map for a generic curve in this family is generically $8:1$ by Proposition 2.31. The branched cover π associated to generic slices of these curves' joint signatures has degree 7584, as opposed to the expected 15480 for generic sextics (see Conjecture 4.2). The monodromy group is a subgroup of $D_8 \wr S_{948}$. We may compute a witness set by collecting one point in each of the 948 disjoint fibers of Φ_p over generic p.

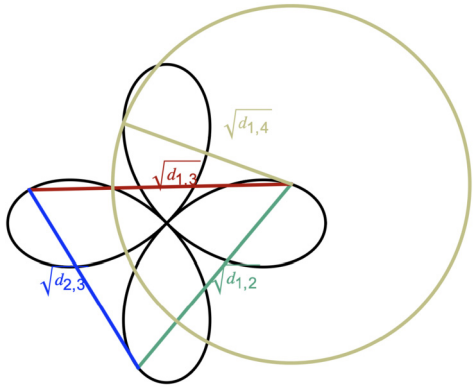

For this family of curves, it is also interesting to consider multiprojective witness sets with multidimension $\mathbf{e}_1$ as in Conjecture 4.2. This means taking coordinate slices where the distances $d_{12}, d_{13}, d_{14}, d_{23}$ are fixed. The associated branched cover has degree 3712 (as opposed to the expected 10080), and the monodromy group is a subgroup of $D_8 \wr (S_8 \wr S_{58})$. The second level of imprimitivity may be explained as follows. For $d_4(p_1, \ldots, p_4) = (d_{12}, d_{14}, \ldots, d_{34})$ generic, there is a circle centered at p_1 of radius $\sqrt{d_{14}}$ which intersects $f(x, y; p) = 0$ in 8 points, as shown in the figure above. Thus, to compute a witness set for the joint signature, it is sufficient to enumerate the fibers of π first by computing 58 witness points up to both the D_8-symmetry and the grouping of points $(p_1, \ldots, p_4)$ with $(p_1, \ldots, p_3)$ equal, and then compute the remaining intersection points of the given curve with the 58 circles.

Finally, we specialize from the case of a generic curve to that of any curve given by $p_1 \in \mathbb{C}^{\binom{d+2}{2}}$ whose signature variety has the expected dimension k. We may then compute a pseudo-witness set for the signature $\Phi_1 = \Phi(\cdots; p_1)$ using the following steps, which are standard in numerical algebraic geometry:

1) Fix generic $(x_0, y_0) \in \mathbb{C}^{2k}$, and find (p_0, L_0) so that $(x, y, p_0, L_0) \in V_\Phi$ by solving linear systems of equations: first in p, then in the parameters defining L.
2) Using the transitivity of the monodromy group, complete (x_0, y_0) to a pseudowitness set for the curve given by p_0 by tracking solution curves along random loops based at (p_0, L_0).

3) By general parameter continuation (Wampler et al., 2005, Theorem 7.1.1 (5)), the pseudowitness set for p_1 will consist of finite, nonsingular endpoints as $t \to 1$ of the homotopy

$$H_p(x;t) = \begin{pmatrix} f_{1,\dots,k}(x, y; tp_1 + (1-t)p_0) \\ L \circ \Phi(x, y; tp_1 + (1-t)p_0) \end{pmatrix} = 0. \tag{8}$$

The same strategy will for more general families, provided that V_Φ is irreducible. For computing witness sets of particular signature maps within a particular family of curves satisfying this condition, we note that Steps 1–2) only need to be performed once.

4. Implementation, examples, and experiments

We run a variety of tests in this section to investigate the numerical stability of our implementation of Algorithm 1. The purpose behind this is two-fold. First we confirm that the implementation will correctly conclude, in most cases, when two curves have the same signature. Secondly we want to answer the question, "What level of perturbation of the curve, or any equivalent curve, will induce a negative result?" Negative here means that the algorithm concludes that the curves have different signatures and thus are *not* equivalent. As mentioned in the introduction, our experiments are motivated by applications in curve-matching where, at best, two curves are only "almost" equivalent under some group action.

Our results showcase features of the `NumericalAlgebraicGeometry` ecosystem in Macaulay2 (aka `NAG4M2`, see Leykin (2011, 2018) for an overview). We rely extensively on the core path-tracker and the packages `SLPexpressions` and `MonodromySolver`. All of our examples and experiments deal with differential and joint signatures for either the Euclidean or equi-affine group.[5] However, the current functionality should make it easy to study other group actions and variations on the signature construction in the future.

The differential signatures for curves under $\mathcal{E}_2(\mathbb{C})$ and $\mathcal{SA}_2(\mathbb{C})$ are defined in Examples 2.21 and 2.22 respectively, and the joint signatures are defined in Definition 2.23 and in (3). To distinguish between the two groups, for a curve C, we denote the Euclidean differential and joint signatures of C as $\mathcal{J}_C^{\mathcal{E}}$ and $\mathcal{S}_C^{\mathcal{E}}$ respectively. Similarly we denote the equi-affine differential and joint signatures of C as $\mathcal{J}_C^{\mathcal{SA}}$ and $\mathcal{S}_C^{\mathcal{SA}}$. We caution that we do not explicitly prove that $\mathcal{J}_C^{\mathcal{SA}}$ characterizes the equivalence class of C under $\mathcal{SA}_2(\mathbb{C})$, as we do for the Euclidean joint signature. However as we explain in Remark 2.34 it is likely that it does.

Our initial attempts to compute witness sets for the both signatures with off-the-shelf tools did not result in consistent monodromy runs for curves of even low degree. Thus, certain choices in our implementation which led to consistent runs, and improved numerical stability, deserve emphasis. Among these choices, a key feature is that polynomials and rational maps are given by straight-line programs as opposed to their coefficient representations. This is especially crucial in the case of differential signatures, where we can do efficient evaluation using the formulas in equation (2); we note that expanding these rational functions in the monomial basis involves many terms and does not suggest a natural evaluation scheme. We also homogenize the equations of our plane curves and work in a random affine chart; the normalizing effect of lifting solutions into projective spaces is known in numerical algebraic geometry, see Bates et al. (2013, Sec. 4.7) for an explanation. Finally, in our sampling procedure we discard samples which map too close to the origin in the codomain of our maps, as these tend to produce nearly-singular points on the image.

Example 4.1. The code below computes a witness set for the Euclidean differential signature of a "generic" quartic (whose coefficients are random complex numbers of modulus 1).

```
(d, k) = (4, 1);
dom = domain(d, k);
```

[5] For details we refer to the code: https://github.com/timduff35/NumericalSignatures.

d	$\deg \mathcal{S}^{\mathcal{E}}$	time (s)	$\deg_{(1,0)} \mathcal{S}^{\mathcal{E}}$	time (s)
2	6	0.3	3	0.1
3	72	2	36	0.5
4	144	9	72	2
5	240	21	120	4
6	360	55	180	7

Fig. 3. Degrees and monodromy timings for differential signatures.

d	$\deg \mathcal{J}^{\mathcal{E}}$	time (s)	$\deg_{\boldsymbol{e}_1} \mathcal{J}^{\mathcal{E}}$	time (s)	$\deg_{\boldsymbol{e}_2} \mathcal{J}^{\mathcal{E}}$	time (s)
2	42	4	24	2	26	2
3	936	33	576	17	696	16
4	3024	139	1920	57	2448	87
5	7440	463	4800	206	6320	276
6	15480	1315	10080	748	13560	791

Fig. 4. Degrees and monodromy timings for joint signatures (see Conjecture 4.2).

```
Map = diffEuclideanSigMap dom;
H = witnessHomotopy(dom, Map);
W = runMonodromy H;
```

To compute a witness set for the differential signature of the Fermat quartic $V(x^4+y^4+z^4) \subset \mathbb{P}(\mathbb{C}^3)$, we use the previous computation.

```
R = QQ[x,y,z];
f=x^4+y^4+z^4;
Wf = witnessCollect(f, W)
```

The output resulting from the last line reads

```
witness data w/ 18 image points (144 preimage points)
```

indicating that the Euclidean differential signature map is generically 8 to 1, which is equivalent to the Fermat curve having eight Euclidean symmetries (Kogan et al., 2020, Thm 2.38). We timed these witness set computations at 5 and 0.5 seconds, respectively. For joint signatures, the analogous computations were timed at 95 and 17 seconds.

Figs. 3 and 4 give degrees and single-run timings for monodromy computations on curves up to degree 6 under the Euclidean differential and joint signatures. We also considered multiprojective witness sets for $\mathcal{S}^{\mathcal{E}} \subset \mathbb{C}^1 \times \mathbb{C}^1$ and $\mathcal{J}^{\mathcal{E}} \subset (\mathbb{C}^1)^6$, where fewer witness points are needed. For the differential signatures, we considered $(1,0)$-slices which fix the value of the squared curvature K_1. For Euclidean joint signatures, there are two combinatorially distinct classes of $(\mathbb{C}^1)^6$ witness sets determined by which $d_{i,j}$ are fixed; the undirected graph of fixed distances must either be the 3-pan (a 3-cycle with pendant edge) or the 4-cycle. We fix corresponding multidimensions $\boldsymbol{e}_1 = (1,1,1,1,0,0)$ and $\boldsymbol{e}_2 = (0,1,1,1,1,0)$.

Our monodromy computations suggested formulas for the degrees and multidegrees of Euclidean joint signatures. To complement the degrees of differential signature curves reported in Kogan et al. (2020), we state these formulas as conjectures. In fact, we have verified these conjectures for d as large as 10, although this was prohibitive in the experimental setup that produced Fig. 4. These formulas for $d=2$ are corrected by a factor of 4, which counts the Euclidean symmetries of a generic conic.

Conjecture 4.2. *Let $\mathcal{J}_d^{\mathcal{E}}$ denote the Euclidean joint signature for a generic plane curve of degree d. For $d \geq 3$:*

$$\deg \overline{\mathcal{J}_d^{\mathcal{E}}} = 12d(d^3-1)$$

d	track time (ms)	lookup time (ms)	track K_1	lookup K_1
2	191	0.35	127	0.25
3	177	0.37	121	0.31
4	276	0.42	145	0.36
5	472	0.39	203	0.43
6	597	0.40	284	0.37

Fig. 5. Equality test timings for Euclidean differential signatures $\mathcal{S}^{\mathcal{E}}$, divided by path-tracking time and time to perform the lookup in line 7 of Algorithm 1. The rightmost columns give the same timings for multiprojective witness sets which fix the first coordinate of the differential signature map.

d	track time (ms)	lookup time (ms)	track $\boldsymbol{e}_1$	lookup $\boldsymbol{e}_1$
2	230	0.36	208	0.34
3	283	0.38	213	0.35
4	335	0.39	288	0.40
5	409	0.32	357	0.32
6	507	0.32	462	0.33

Fig. 6. Equality test timings for Euclidean joint signatures $\mathcal{J}^{\mathcal{E}}$.

$$\deg_{\boldsymbol{e}_1} \mathcal{J}_d^{\mathcal{E}} = 8d^2(d^2-1)$$
$$\deg_{\boldsymbol{e}_2} \mathcal{J}_d^{\mathcal{E}} = 4d(d-1)(3d^2+d-1).$$

To assess the speed and robustness of the online equality test, we conducted an experiment where, for degrees $d = 2, \ldots, 6$, curves $C_1, \ldots, C_{10}$ were generated with coefficients drawn uniformly from the unit sphere in $\mathbb{R}^{(d+2)(d+1)/2}$. For each C_i, we computed a witness set via parameter homotopy from a generic degree d curve. We then applied 20 random transformations from $\mathcal{E}_2(\mathbb{R})$ to the C_i and perturbed the resulting coefficients by random real $\vec{\epsilon}$ with $\|\vec{\epsilon}\|_2 \in \{0, 10^{-7}, 10^{-6}, \ldots, 10^{-3}\}$, thus obtaining curves $\widetilde{C_{i,1,\epsilon}}, \ldots, \widetilde{C_{i,20,\epsilon}}$. Thus two curves are "close" if they are close in the space of algebraic curves of fixed degree with respect to $||\cdot||_2$, and the curves C_i and C_j are "almost" equivalent if C_i is $\mathcal{E}_2(\mathbb{R})$-equivalent to a curve that is "close" to C_j. With all numerical tolerances fixed, we ran the equality test for each $\widetilde{C_{i,j,\epsilon}}$ against each C_i.

Figs. 5 and 6 summarize the timings for the equality tests in this experiment. Overall, these tests run on the order of sub-seconds. Most of the time is spent on path-tracking. The tracking times reported give the total time spent on lines 1 and 6 of Algorithm 1. The only other possible bottleneck is the lookup on line 7. This is negligible, even for large witness set sizes, if an appropriate data structure is used. The runtimes for all cases considered seem comparable, although using differential signatures and multiprojective slices appear to give a slight edge over the respective alternatives.

The plots in Fig. 7 illustrate the results of our sensitivity analysis. The respective axes are the magnitude of the noise ϵ and the percentage of $C_{i,j,\epsilon}$ deemed to be not equivalent to C_i. Note that the horizontal axis is given on a log scale, and excludes the noiseless case $\epsilon = 0$; for this case, among all tests in the experiment, only one false negative was reported for the differential signatures with $d = 6$. We include a trend line to make the plots more readable. In general, we observe a threshold phenomenon, where most tests are positive for sufficiently low noise and are negative for sufficiently high noise. Besides the multiprojective differential signature (depicted in the bottom-left), we observe a similar stability profile for this type of random perturbation.

Remark 4.3. The thresholds in these experiments clearly depend on the numerical tolerances used (for this experiment, defaults are provided by `NAG4M2`), the type of map, and the type of witness set.

In Fig. 8, we reproduce the previous experiment for curves of degrees $d = 3, 4, 5$ under $\mathcal{SA}_2(\mathbb{C})$. Perhaps unsurprisingly due to the higher degree of the image and the complexity of evaluating the signature maps, the equality test in this case is much more sensitive to small perturbations. Here we observe a significant difference in the sensitivity between the equi-affine joint and differential equality

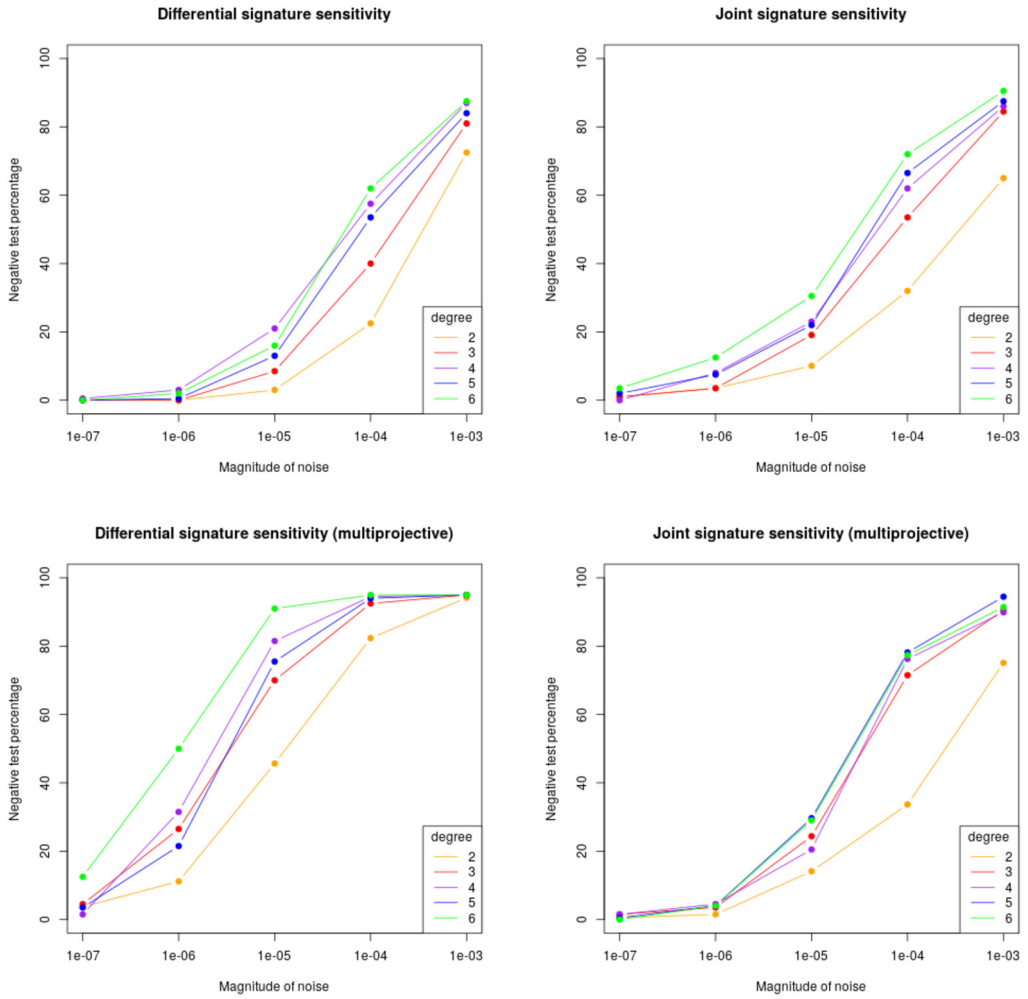

Fig. 7. Sensitivity of the equality test on Euclidean signatures to noise.

tests. In contrast to the Euclidean case, the joint signature appears to be *far less* sensitive. We also now observe in around 2% of cases overall that there are *failures* due to path-tracking, resulting in neither an equivalent nor inequivalent outcome. We again exclude the noiseless case $\epsilon = 0$ in these graphs where the false negative rate was less than 1%. Surprisingly, we also observed a non-negligible rate of "false-positives" for the $\mathcal{SA}_2(\mathbb{C})$ joint signature, wherein some C_i and C_j are declared equivalent. We also note that we do not have an analogue of Conjecture 4.2 for $\mathcal{J}^{\mathcal{SA}}$, leaving us less certain about the completeness of the witness sets collected.

In our previous experiments we perturbed curves in the space of algebraic curves of fixed degree. Here we conduct a similar experiment for the Euclidean differential and joint signatures under a different scheme of noise inspired by applications such as curve-matching (Hoff and Olver, 2013). Instead of perturbing the coefficients of the algebraic curve, we sample $\binom{d+2}{2}+1$ points on curves $C_1, \ldots, C_{10}$, perturb these points by $\vec{\epsilon} \in \mathbb{R}^2$ with $|\vec{\epsilon}| = \epsilon$, and then reconstruct a new algebraic curve of the same degree through *interpolation* before applying a random transformation from $\mathcal{E}_2(\mathbb{R})$. Specifically, the equation defining our interpolated curve comes from singular vectors of the *Vandermonde*

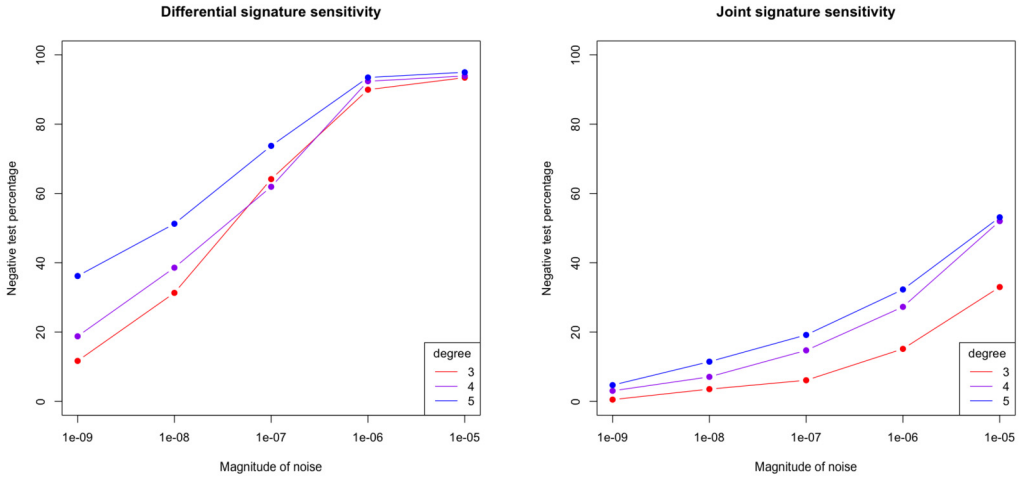

Fig. 8. Sensitivity of the equality test on equi-affine signatures to noise.

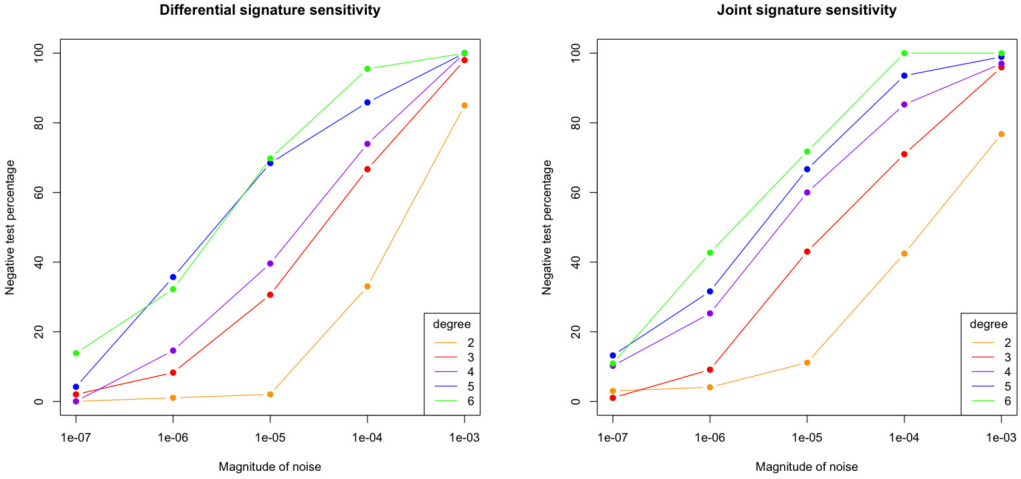

Fig. 9. Sensitivity of the equality test for Euclidean signatures of curves computed from noisy samples.

matrix of all degree-$\leq d$ monomials evaluated at the samples, as in Breiding et al. (2018). Now a curve C_j is "close" to C_i if the samples taken from C_i nearly lie on C_j, and the curves C_i and C_j are "almost" equivalent if C_j is $\mathcal{E}_2(\mathbb{R})$-equivalent to a curve that is "close" to C_i. We emphasize that the coefficients of the perturbed curves have a more complicated dependence on ϵ in this experiment. Moreover, we caution that our results may also depend on the number of points sampled from each curve. Still, we find that the observations from this new experiment, with a more meaningful model of noise, and our original experiment are roughly consistent. (See Fig. 9.)

In closing, we have shown that numerical algebraic geometry is a novel and effective tool for studying signatures and the group valence problem. Our results suggest new avenues of mathematical research and our experimental results contribute to the ongoing study of signatures of curves under noise. In general, we found that using numerical algebraic geometry and signatures to determine equivalence of algebraic curves can be sensitive to a moderate amount of noise. However, we have only taken first steps towards exploring this topic and its applications, and we hope our efforts motivate future work.

Declaration of competing interest

The authors declare that they have no known competing financial interests or personal relationships that could have appeared to influence the work reported in this paper.

Acknowledgements

T. Duff acknowledges support from an NSF Mathematical Sciences Postdoctoral Research Fellowship (DMS-2103310), as well as past support from NSF DMS-1719968, a fellowship from the Algorithms and Randomness Center at Georgia Tech, the Max Planck Institute for Mathematics in the Sciences in Leipzig while this work was in progress. Research of M. Ruddy was supported in part by the Max Planck Institute for Mathematics in the Sciences in Leipzig. We thank an anonymous reviewer for several suggestions that led to greatly improving the final manuscript.

References

Allgower, E.L., Georg, K., 1990. Numerical Continuation Methods: An Introduction, vol. 13. Springer Science & Business Media.
Améndola, C., Lindberg, J., Rodriguez, J.I., 2021. Solving parameterized polynomial systems with decomposable projections. arXiv preprint, arXiv:1612.08807.
Bates, D.J., Hauenstein, J.D., Sommese, A.J., Wampler, C.W., 2013. Numerically Solving Polynomial Systems with Bertini. SIAM.
Berchenko (Kogan), I.A., Olver, P.J., 2000. Symmetries of polynomials. J. Symb. Comput. 29, 485–514.
Breiding, P., Kališnik, S., Sturmfels, B., Weinstein, M., 2018. Learning algebraic varieties from samples. Rev. Mat. Complut. 31 (3), 545–593.
Brysiewicz, T., 2018. Numerical software to compute Newton polytopes and tropical membership. In: International Congress on Mathematical Software. Springer, pp. 80–88.
Burdis, J.M., Kogan, I.A., Hong, H., 2013. Object-image correspondence for algebraic curves under projections. SIGMA 9, 023.
Calabi, E., Olver, P.J., Shakiban, C., Tannenbaum, A., Haker, S., 1998. Differential and numerically invariant signatures curves applied to object recognition. Int. J. Comput. Vis. 26 (2), 107–135.
Chen, J., Kileel, J., 2019. Numerical implicitization. J. Softw. Algebra Geom. 9, 55–65.
Derksen, H., Kemper, G., 2015. Computational Invariant Theory, enlarged ed. Encyclopaedia of Mathematical Sciences, vol. 130. Springer, Heidelberg.
Duff, T., Hill, C., Jensen, A., Lee, K., Leykin, A., Sommars, J., 2019. Solving polynomial systems via homotopy continuation and monodromy. IMA J. Numer. Anal. 39 (3), 1421–1446.
Duff, T., Ruddy, M., 2020. Numerical equality tests for rational maps and signatures of curves. In: Proceedings of the 45th International Symposium on Symbolic and Algebraic Computation. ACM.
Fels, M., Olver, P.J., 1999. Moving coframes. II. Regularization and theoretical foundations. Acta Appl. Math. 55 (2), 127–208.
Grayson, D., Stillman, M., 1997. Macaulay2—a system for computation in algebraic geometry and commutative algebra.
Grim, A., Shakiban, C., 2017. Applications of signature curves to characterize melanomas and moles. In: Applications of Computer Algebra. In: Springer Proc. Math. Stat., vol. 198. Springer, Cham, pp. 171–189.
Guggenheimer, H.W., 1963. Differential Geometry. McGraw-Hill Book Co., Inc., New York-San Francisco-Toronto-London.
Harris, J., 2013. Algebraic Geometry: A First Course, vol. 133. Springer Science & Business Media.
Hauenstein, J.D., Leykin, A., Rodriguez, J.I., Sottile, F., 2022. A numerical toolkit for multiprojective varieties. Math. Comput. 90 (327), 413–440.
Hauenstein, J.D., Regan, M.H., 2020. Evaluating and differentiating a polynomial using a pseudo-witness set. In: International Congress on Mathematical Software. Springer, pp. 61–69.
Hauenstein, J.D., Rodriguez, J.I., 2020. Multiprojective witness sets and a trace test. Adv. Geom. 20 (3), 297–318.
Hauenstein, J.D., Sommese, A.J., 2010. Witness sets of projections. Appl. Math. Comput. 217 (7), 3349–3354.
Hauenstein, J.D., Sommese, A.J., 2013. Membership tests for images of algebraic sets by linear projections. Appl. Math. Comput. 219 (12), 6809–6818.
Hauenstein, J.D., Sottile, F., 2014. Newton polytopes and witness sets. Math. Comput. Sci. 8 (2), 235–251.
Hoff, D.J., Olver, P.J., 2013. Extensions of invariant signatures for object recognition. J. Math. Imaging Vis. 45 (2), 176–185.
Hoff, D.J., Olver, P.J., 2014. Automatic solution of jigsaw puzzles. J. Math. Imaging Vis. 49 (1), 234–250.
Hubert, E., Kogan, I.A., 2007. Smooth and algebraic invariants of a group action: local and global construction. Found. Comput. Math. J. 7 (4), 345–383.
Kogan, I.A., Moreno Maza, M., 2002. Computation of canonical forms for ternary cubics. In: Proceedings of the 2002 International Symposium on Symbolic and Algebraic Computation. ACM, New York, pp. 151–160.
Kogan, I.A., Ruddy, M., Vinzant, C., 2020. Differential signatures of algebraic curves. SIAM J. Appl. Algebra Geom. 4 (1), 185–226.
Leykin, A., 2011. Numerical algebraic geometry. J. Softw. Algebra Geom. 3 (1), 5–10.
Leykin, A., 2018. Homotopy continuation in Macaulay2. In: International Congress on Mathematical Software. Springer, pp. 328–334.
Leykin, A., Rodriguez, J.I., Sottile, F., 2018. Trace test. Arnold Math. J. 4 (1), 113–125.
Monagan, M., Pearce, R., 2006. Rational simplification modulo a polynomial ideal. In: ISSAC 2006. ACM, New York, pp. 239–245.

Morgan, A., 2009. Solving Polynomial Systems Using Continuation for Engineering and Scientific Problems, vol. 57. SIAM.
Morgan, A.P., Sommese, A.J., 1989. Coefficient-parameter polynomial continuation. Appl. Math. Comput. 29 (2), 123–160.
Mundy, J.L., Zisserman, A., Forsyth, D. (Eds.), 1994. Applications of Invariance in Computer Vision. Springer, Berlin, Heidelberg.
Olver, P.J., 1995. Equivalence, Invariants and Symmetry. Cambridge University Press.
Olver, P.J., 1999. Classical Invariant Theory. London Mathematical Society Student Texts, vol. 44. Cambridge University Press, Cambridge.
Olver, P.J., 2001. Joint invariant signatures. Found. Comput. Math. 1 (1), 3–67.
Ruddy, M., 2019. The Equivalence Problem and Signatures of Algebraic Curves. PhD thesis. North Carolina State University.
Shafarevich, I., 1994. Basic Algebraic Geometry, vol. 2, 2nd ed. Springer.
Sommese, A.J., Verschelde, J., Wampler, C.W., 2005. Introduction to numerical algebraic geometry. In: Solving Polynomial Equations. Springer, pp. 301–337.
Sturmfels, B., 2008. Algorithms in Invariant Theory. Springer, Vienna.
Wampler, I.C.W., et al., 2005. The Numerical Solution of Systems of Polynomials Arising in Engineering and Science. World Scientific.